SWISS CONTRIBUTION

NANOSPIN

Measurement of transverse spin penetration length using second harmonic voltage

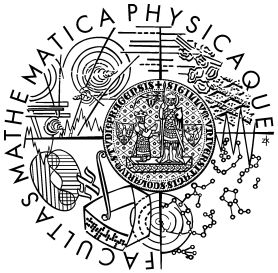

Pavel Baláž

Charles University, Faculty of Mathematics and Physics
Department of Condensed Matter Physics
Prague, Czech Republic

11–12 July 2016, Nanospin Summarizing Meeting, Kraków, Poland

1. Playing with second harmonic
2. Phase transitions in Mn-doped 3D topological insulators
3. Laser-pulse-induced ultrafast spin transport

Outline

Model

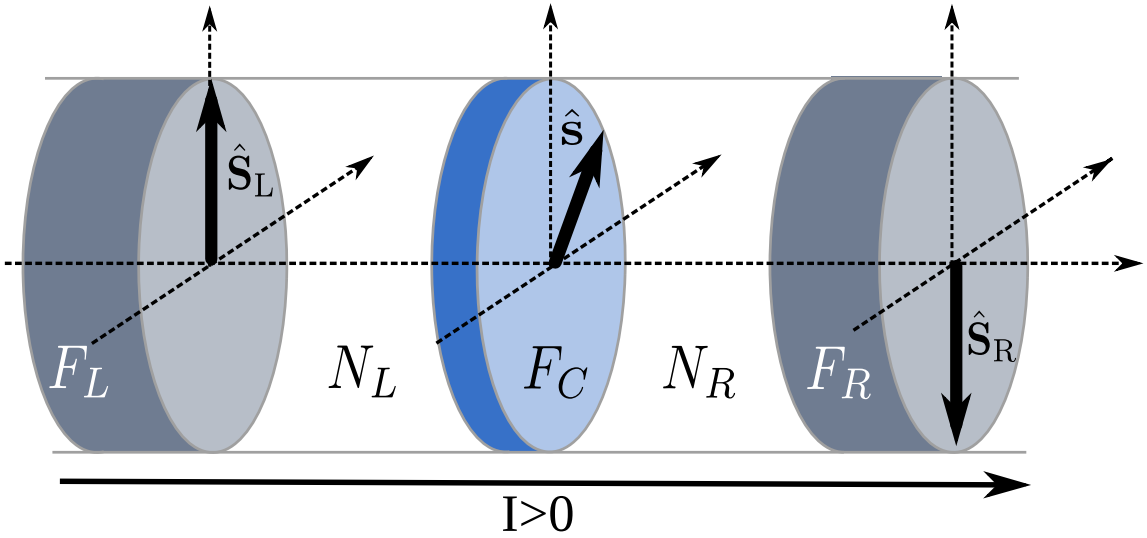
$\hat{\mathbf{S}}_L$
$\hat{\mathbf{s}}$
$\hat{\mathbf{S}}_R$
F_L
N_L
F_C
N_R
F_R
I>0

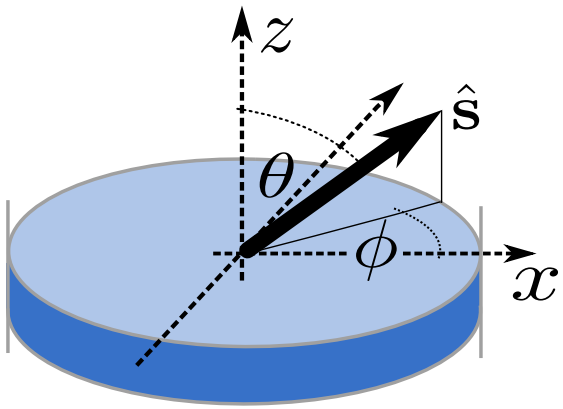
z
$\hat{\mathbf{s}}$
θ
ϕ
x

Previous study

- Diffusion model $\frac{\mathrm{d}\boldsymbol{f}}{\mathrm{d}t} = \frac{J}{\hbar}\left(\hat{\boldsymbol{S}} \times \boldsymbol{f}\right) + \frac{\partial \boldsymbol{j}}{\partial x} + \frac{\boldsymbol{f}}{\tau_{\mathrm{sf}}}$, where spin distribution function $\boldsymbol{f} = (f_x, f_y, f_z)$ and spin current $\boldsymbol{j} = (j_x, j_y, jz)$
- Transverse spin penetration length, λ_t, is a parameter of the model

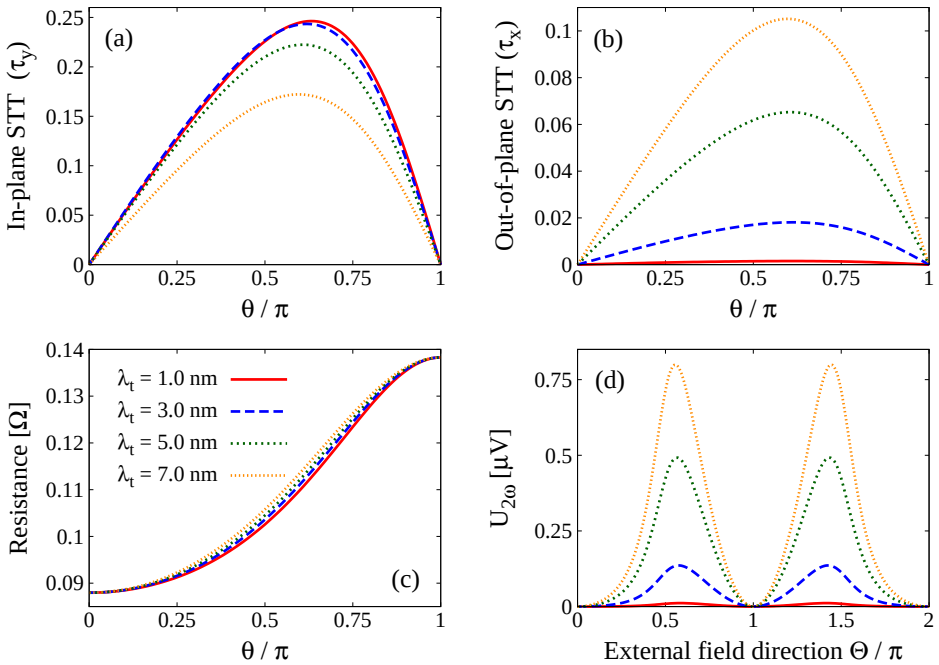

P. Baláž, J. Barnaś, and J.-Ph. Ansermet
Transverse spin penetration length in metallic spin valves
J. Appl. Phys. **113**, 193905 (2013)

Transport through and ultrathin magnetic layer

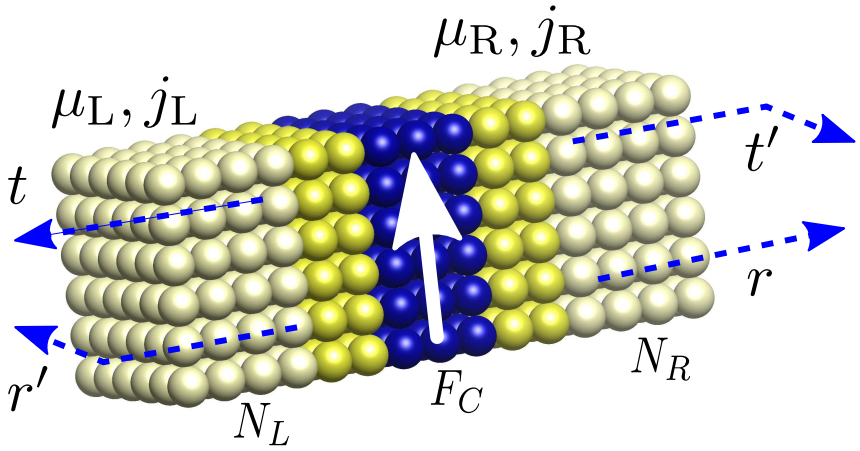

From *ab initio*:

- Sharvin conductance: G_{Sh}
- Channel resistivities: $R_{\uparrow(\downarrow)} = {G_{\uparrow(\downarrow)}}^{-1}$
- Mixing conductance: $G_{\uparrow\downarrow} = g_{\mathrm{r}} + i\, g_{\mathrm{i}}$
- Mixing transmission: $T_{\uparrow\downarrow} = t_{\mathrm{r}} + i\, t_{\mathrm{i}}$

transverse spin current

$$\boldsymbol{j}_{\perp\mathrm{L}} = \begin{pmatrix} j_{x\mathrm{L}} \\ j_{y\mathrm{L}} \end{pmatrix}, \boldsymbol{j}_{\perp\mathrm{R}} = \begin{pmatrix} j_{x\mathrm{R}} \\ j_{y\mathrm{R}} \end{pmatrix}$$

transverse spin accumulation

$$\boldsymbol{\mu}_{\perp\mathrm{L}} = \begin{pmatrix} \mu_{x\mathrm{L}} \\ \mu_{y\mathrm{L}} \end{pmatrix}, \boldsymbol{\mu}_{\perp\mathrm{R}} = \begin{pmatrix} \mu_{x\mathrm{R}} \\ \mu_{y\mathrm{R}} \end{pmatrix}$$

Boundary condition

$$\begin{pmatrix} \boldsymbol{j}_{\perp\mathrm{R}} \\ \boldsymbol{j}_{\perp\mathrm{L}} \end{pmatrix} = \begin{pmatrix} -\boldsymbol{G} & -\boldsymbol{T} \\ \boldsymbol{T} & \boldsymbol{G} \end{pmatrix} \begin{pmatrix} \boldsymbol{\mu}_{\perp\mathrm{R}} \\ \boldsymbol{\mu}_{\perp\mathrm{L}} \end{pmatrix}$$

where

$$\boldsymbol{G} = 2 \begin{pmatrix} -g_{\mathrm{r}} & g_{\mathrm{i}} \\ -g_{\mathrm{i}} & -g_{\mathrm{r}} \end{pmatrix} \text{ and } \boldsymbol{T} = 2 \begin{pmatrix} t_{\mathrm{r}} & -t_{\mathrm{i}} \\ t_{\mathrm{i}} & t_{\mathrm{r}} \end{pmatrix}$$

Second harmonic response voltage

Spin transfer toque

$$\boldsymbol{\tau} = \frac{\hbar}{2}\left(\boldsymbol{j}_{\perp \mathrm{L}} - \boldsymbol{j}_{\perp \mathrm{R}}\right)$$

In-plane torque: $\boldsymbol{\tau}_{\parallel} = I\, a\, \hat{\boldsymbol{s}} \times \left(\hat{\boldsymbol{s}} \times \hat{\boldsymbol{S}}\right)$

Out-of-plane torque: $\boldsymbol{\tau}_{\perp} = I\, b\, \hat{\boldsymbol{s}} \times \hat{\boldsymbol{S}}$

where

$$a = -\frac{\hbar}{2\,I}\,\frac{j_{y\mathrm{L}} - j_{y\mathrm{R}}}{\sin\xi}, \text{ and } b = \frac{\hbar}{2\,I}\,\frac{j_{x\mathrm{L}} - j_{x\mathrm{R}}}{\sin\xi}$$

or in terms of spin accumulation

$$a = \frac{\hbar}{e^2\,I}\,\frac{a_{\mathrm{r}}\,\mu_y + a_{\mathrm{i}}\,\mu_x}{\sin\xi}$$

$$b = -\frac{\hbar}{e^2\,I}\,\frac{a_{\mathrm{r}}\,\mu_x - a_{\mathrm{i}}\,\mu_y}{\sin\xi}$$

with $A_{\uparrow\downarrow} = G_{\uparrow\downarrow} - T_{\uparrow\downarrow} = a_{\mathrm{r}} + i\,a_{\mathrm{i}}$, and ξ is an angle between $\hat{\boldsymbol{s}}$ and $\hat{\boldsymbol{S}}$.

Second harmonic response voltage

Spin transfer toque

$$\boldsymbol{\tau} = \frac{\hbar}{2}\left(\boldsymbol{j}_{\perp \mathrm{L}} - \boldsymbol{j}_{\perp \mathrm{R}}\right)$$

In-plane torque: $\boldsymbol{\tau}_{\parallel} = I\, a\, \hat{\boldsymbol{s}} \times \left(\hat{\boldsymbol{s}} \times \hat{\boldsymbol{S}}\right)$

Out-of-plane torque: $\boldsymbol{\tau}_{\perp} = I\, b\, \hat{\boldsymbol{s}} \times \hat{\boldsymbol{S}}$

where

$$a = -\frac{\hbar}{2\,I}\,\frac{j_{y\mathrm{L}} - j_{y\mathrm{R}}}{\sin\xi}, \text{ and } b = \frac{\hbar}{2\,I}\,\frac{j_{x\mathrm{L}} - j_{x\mathrm{R}}}{\sin\xi}$$

or in terms of spin accumulation

$$a = a_{\mathrm{r}}\,\frac{\hbar}{e^2\,I}\,\frac{\mu_y}{\sin\xi}$$

$$b = a_{\mathrm{i}}\,\frac{\hbar}{e^2\,I}\,\frac{\mu_y}{\sin\xi}$$

with $A_{\uparrow\downarrow} = G_{\uparrow\downarrow} - T_{\uparrow\downarrow} = a_{\mathrm{r}} + i\,a_{\mathrm{i}}$, and ξ is an angle between $\hat{s}$ and $\hat{S}$. Additionaly, $\mu_x \ll \mu_y$.

Second harmonic response voltage

Spin transfer toque

$$\boldsymbol{\tau} = \frac{\hbar}{2}\left(\boldsymbol{j}_{\perp \mathrm{L}} - \boldsymbol{j}_{\perp \mathrm{R}}\right)$$

In-plane torque: $\boldsymbol{\tau}_{\parallel} = I\, a\, \hat{\boldsymbol{s}} \times \left(\hat{\boldsymbol{s}} \times \hat{\boldsymbol{S}}\right)$

Out-of-plane torque: $\boldsymbol{\tau}_{\perp} = I\, b\, \hat{\boldsymbol{s}} \times \hat{\boldsymbol{S}}$

where

$$a = -\frac{\hbar}{2\,I}\,\frac{j_{y\mathrm{L}} - j_{y\mathrm{R}}}{\sin\xi}, \text{ and } b = \frac{\hbar}{2\,I}\,\frac{j_{x\mathrm{L}} - j_{x\mathrm{R}}}{\sin\xi}$$

or in terms of spin accumulation

$$a = a_{\mathrm{r}}\,\frac{\hbar}{e^2\,I}\,\frac{\mu_y}{\sin\xi}$$

$$b = a_{\mathrm{i}}\,\frac{\hbar}{e^2\,I}\,\frac{\mu_y}{\sin\xi}$$

with $A_{\uparrow\downarrow} = G_{\uparrow\downarrow} - T_{\uparrow\downarrow} = a_{\mathrm{r}} + i\,a_{\mathrm{i}}$, and ξ is an angle between $\hat{\boldsymbol{s}}$ and $\hat{\boldsymbol{S}}$. Additionaly, $\mu_x \ll \mu_y$.

Second harmonic

$$U_{2\omega} = -\frac{I_0^2}{4}\frac{\partial R}{\partial \nu}\,|_{\phi_0}\,\sin\phi_0\,|\chi_\phi|$$

with susceptibility $\chi_\phi(\phi_0, \Theta)$

In the limit of small current frequency

$$\chi_\phi(\phi_0, \Theta) = \frac{|\gamma_{\mathrm{g}}|}{M_{\mathrm{s}}\,d}\,\frac{b_0}{\omega_2(\phi_0, \Theta)}\,\sin\phi_0$$

where b_0 is out-of-plane torque magnitude in the equilibrium point, ϕ_0

Second harmonic response voltage

Spin transfer toque

$$\boldsymbol{\tau} = \frac{\hbar}{2}\left(\boldsymbol{j}_{\perp \mathrm{L}} - \boldsymbol{j}_{\perp \mathrm{R}}\right)$$

In-plane torque: $\boldsymbol{\tau}_{\parallel} = I\, a\, \hat{\boldsymbol{s}} \times \left(\hat{\boldsymbol{s}} \times \hat{\boldsymbol{S}}\right)$

Out-of-plane torque: $\boldsymbol{\tau}_{\perp} = I\, b\, \hat{\boldsymbol{s}} \times \hat{\boldsymbol{S}}$

where

$$a = -\frac{\hbar}{2\,I}\,\frac{j_{y\mathrm{L}} - j_{y\mathrm{R}}}{\sin\xi}, \text{ and } b = \frac{\hbar}{2\,I}\,\frac{j_{x\mathrm{L}} - j_{x\mathrm{R}}}{\sin\xi}$$

or in terms of spin accumulation

$$a = a_{\mathrm{r}}\,\frac{\hbar}{e^2\,I}\,\frac{\mu_y}{\sin\xi}$$

$$b = a_{\mathrm{i}}\,\frac{\hbar}{e^2\,I}\,\frac{\mu_y}{\sin\xi}$$

with $A_{\uparrow\downarrow} = G_{\uparrow\downarrow} - T_{\uparrow\downarrow} = a_{\mathrm{r}} + i\,a_{\mathrm{i}}$, and ξ is an angle between $\hat{\boldsymbol{s}}$ and $\hat{\boldsymbol{S}}$. Additionaly, $\mu_x \ll \mu_y$.

Second harmonic

$$U_{2\omega} = -\frac{I_0^2}{4}\frac{\partial R}{\partial \nu}\,|_{\phi_0}\,\sin\phi_0\,|\chi_\phi|$$

with susceptibility $\chi_\phi(\phi_0, \Theta)$

In the limit of small current frequency

$$\chi_\phi(\phi_0, \Theta) = \frac{|\gamma_{\mathrm{g}}|}{M_{\mathrm{s}}\,d}\,\frac{b_0}{\omega_2(\phi_0, \Theta)}\,\sin\phi_0$$

where b_0 is out-of-plane torque magnitude in the equilibrium point, ϕ_0

Result

$$U_{2\omega} \sim b \sim \mathrm{Im}\{A_{\uparrow\downarrow}\}$$

Cu/Co dual spin valve

ab initio results

Cu – Co(8) ↑ | Cu(5) | Co(d) ↗ | Cu(5) | Co(8) ↓ – Cu

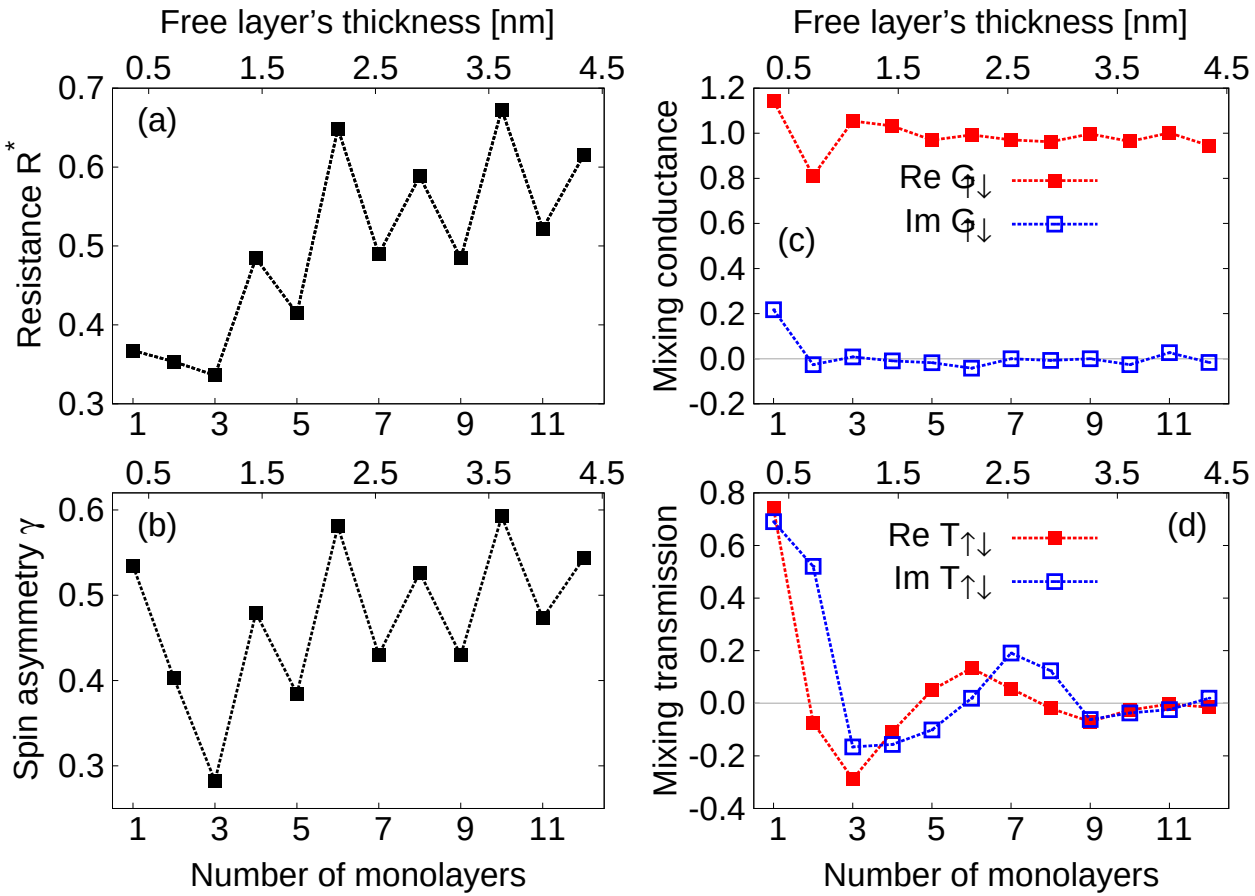

Cu/Co dual spin valve

Spin transfer torque, magnetoresistance, and second harmonics

Cu – Co(8) ↑ | Cu(5) | Co(d) ↗ | Cu(5) | Co(8) ↓ – Cu

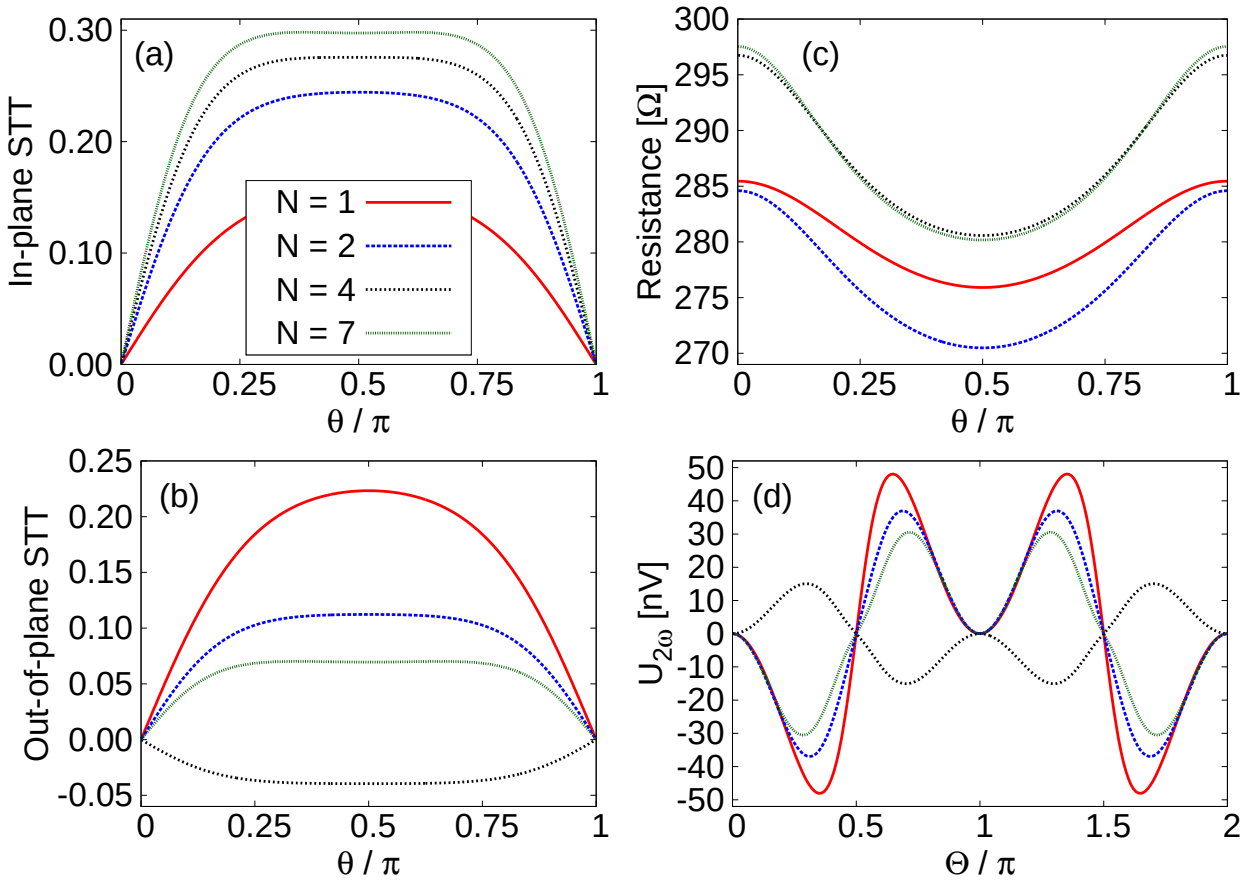

Cu/Co dual spin valve

Second harmonic voltage *vs.* $\mathrm{Im}A_{\uparrow\downarrow}$

Cu – Co(8) ↑ | Cu(5) | Co(d) ↗ | Cu(5) | Co(8) ↓ – Cu

clean interfaces

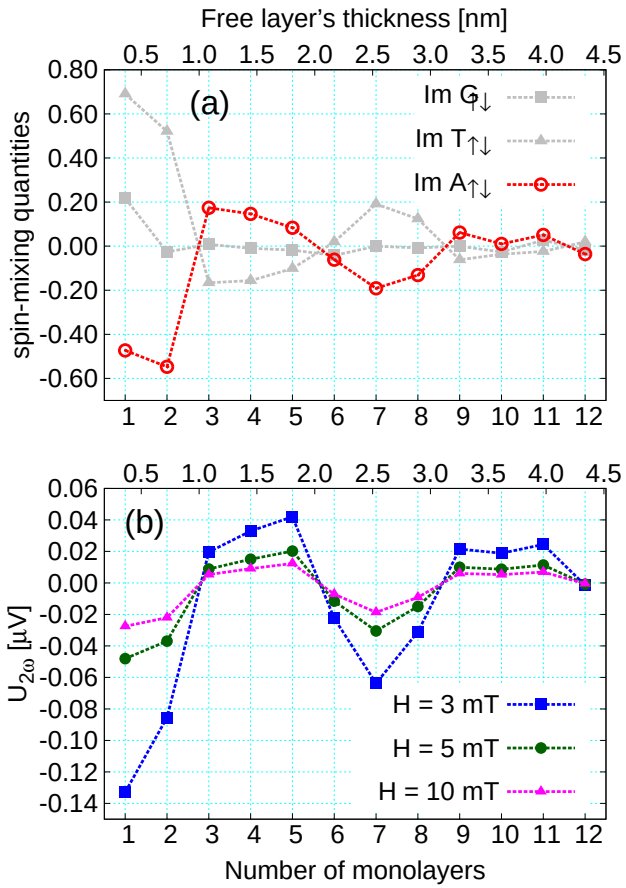

Cu/Co dual spin valve

Second harmonic voltage *vs.* $\mathrm{Im}A_{\uparrow\downarrow}$

Cu – Co(8) ↑ | Cu(5) | Co(d) ↗ | Cu(5) | Co(8) ↓ – Cu

clean interfaces

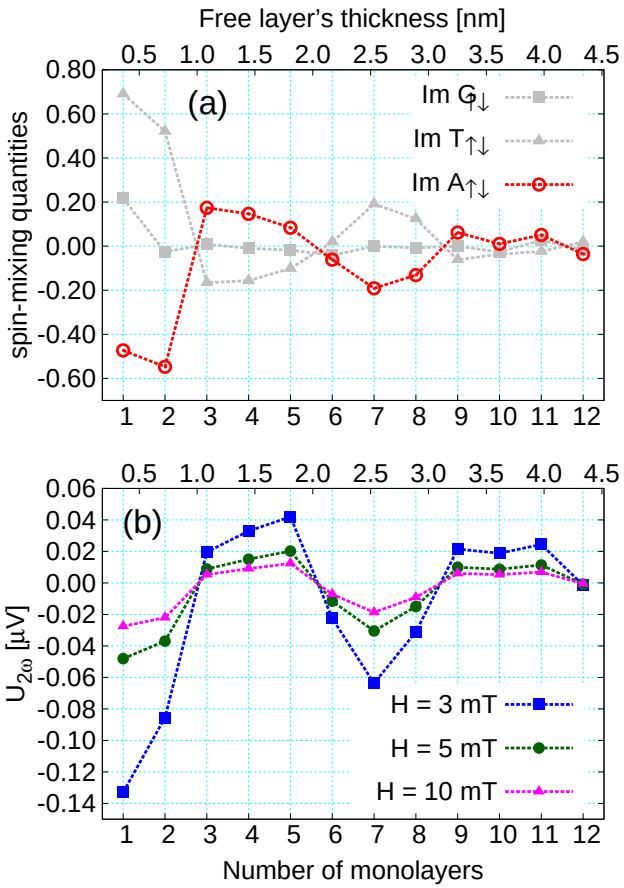

effect of interface disorder

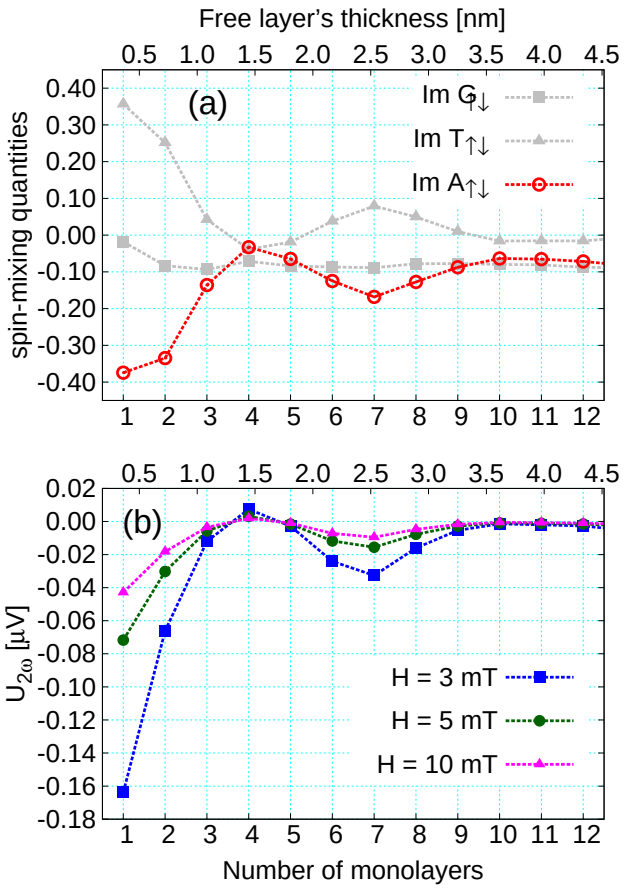

Cu/Ni dual spin valve

Second harmonic voltage *vs.* $\mathrm{Im}A_{\uparrow\downarrow}$

Cu – Ni(8) ↑ | Cu(5) | Ni(d) ↗ | Cu(5) | Ni(8) ↓ – Cu

clean interfaces

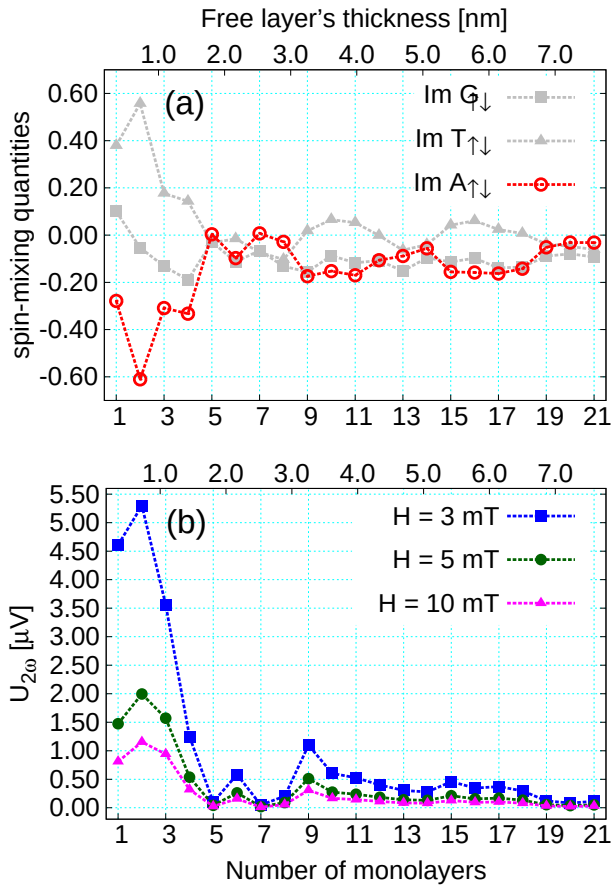

Cu/Ni dual spin valve

Second harmonic voltage *vs.* $\mathrm{Im}A_{\uparrow\downarrow}$

Cu – Ni(8) ↑ Cu(5) Ni(d) ↗ Cu(5) Ni(8) ↓ – Cu

clean interfaces

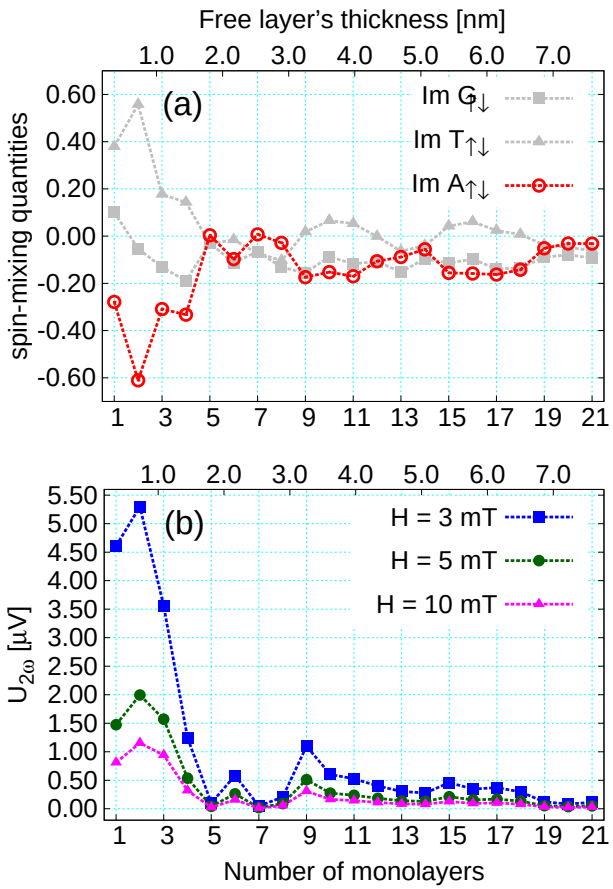

effect of interface disorder

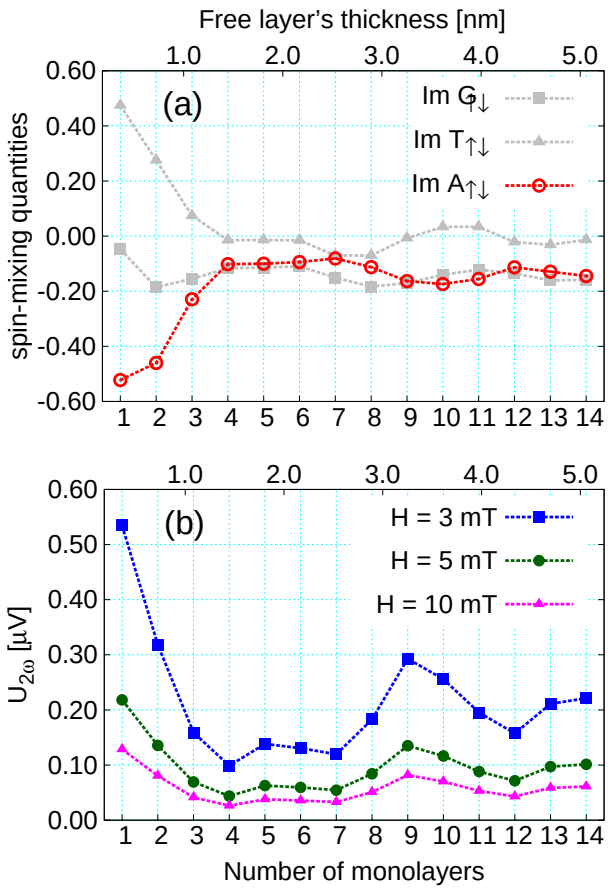

Au/Fe dual spin valve

Second harmonic voltage *vs.* $\mathrm{Im}A_{\uparrow\downarrow}$

Au – Co(8) ↑ | Au(5) | Fe(d) ↗ | Au(5) | Co(8) ↓ – Au

clean interfaces

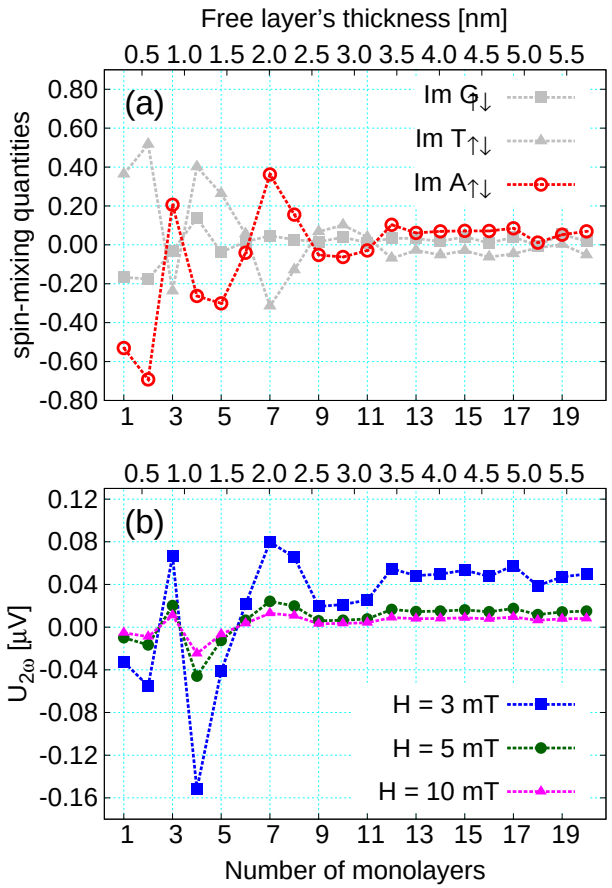

Au/Fe dual spin valve

Second harmonic voltage *vs.* $\mathrm{Im}A_{\uparrow\downarrow}$

Au – Co(8) ↑ | Au(5) | Fe(d) ↗ | Au(5) | Co(8) ↓ – Au

clean interfaces

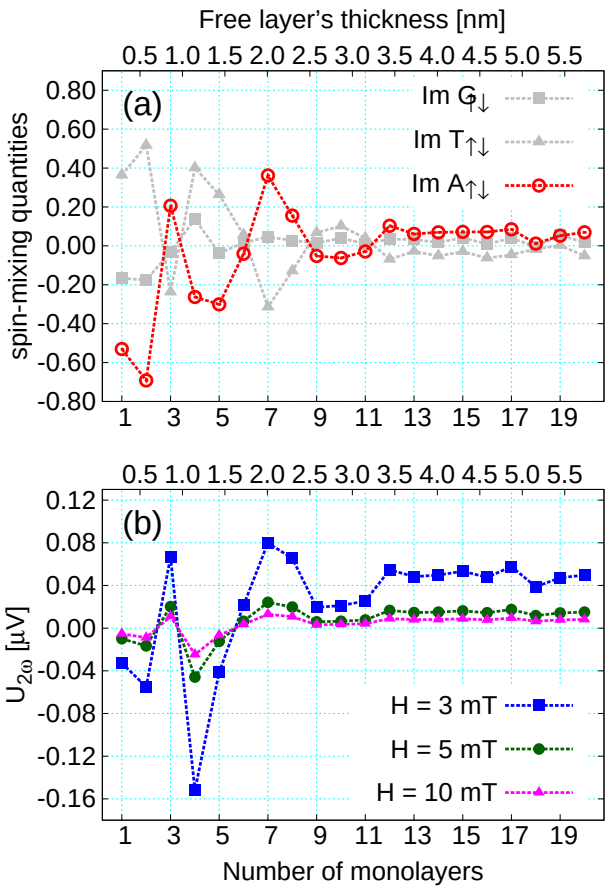

effect of interface disorder

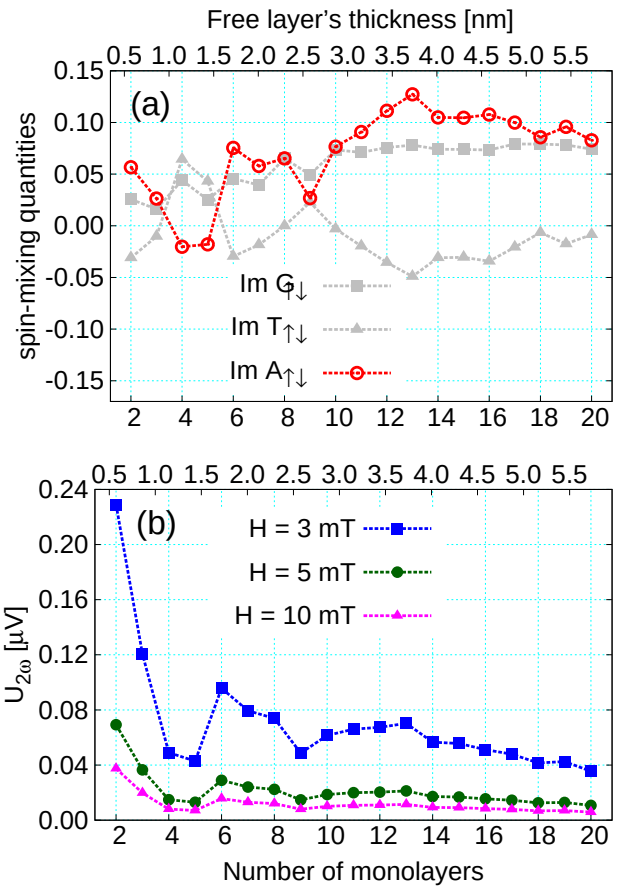

Summary

for calculations of second harmonic response voltage

- Measurement of second harmonic voltage can be used to estimate out-of-plane spin torque component.
- We have shown correlations between second harmonic voltage and $\mathrm{Im}A_{\uparrow\downarrow}$.
- Using second harmonics voltage measurement one can define transverse spin penetration length.

Outline

3D topological insulators Bi_2Te_3 and Bi_2Se_3

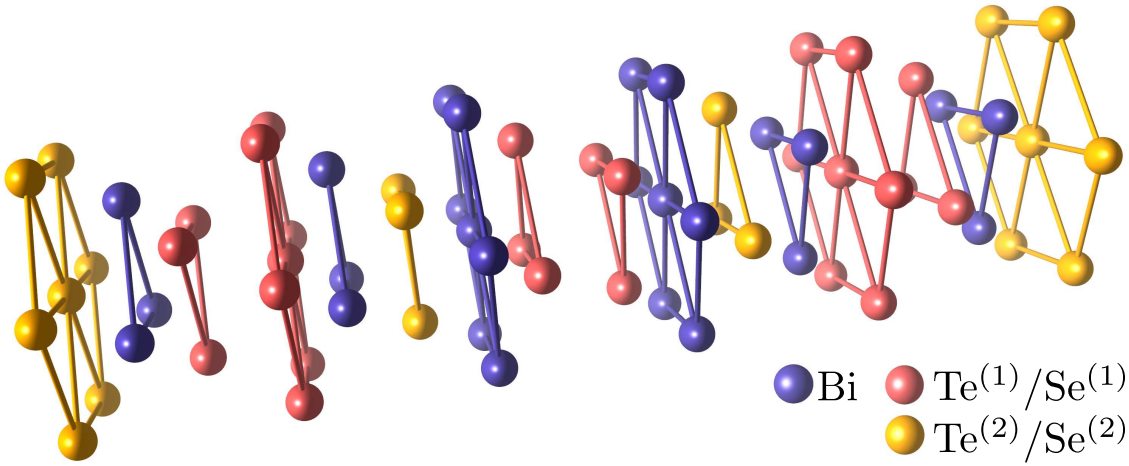

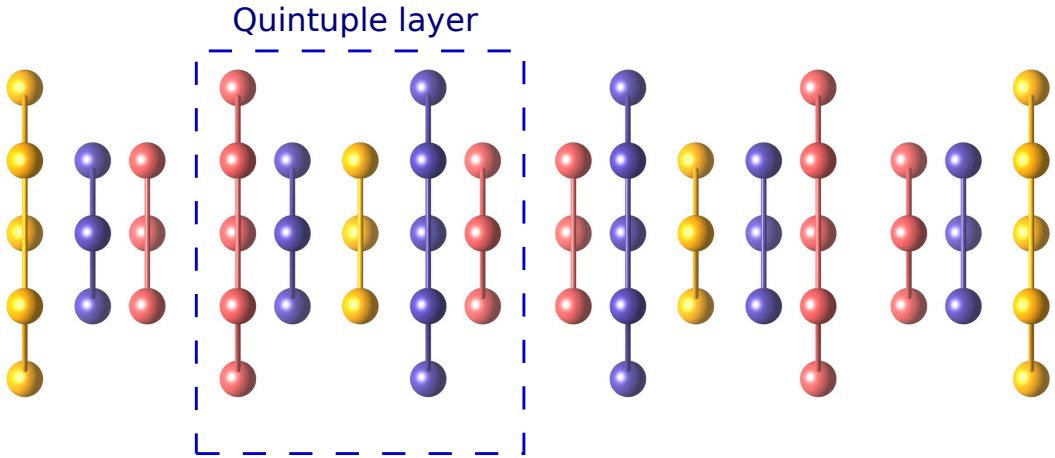

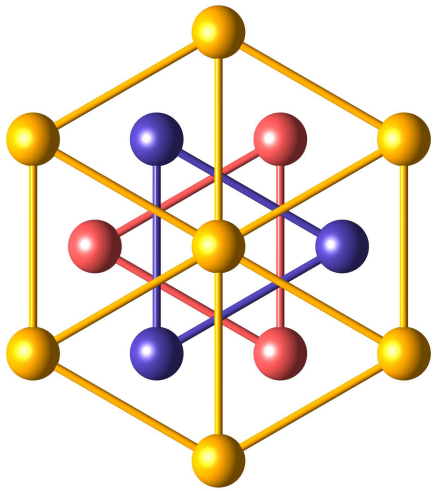

3D topological insulators Bi_2Te_3 and Bi_2Se_3

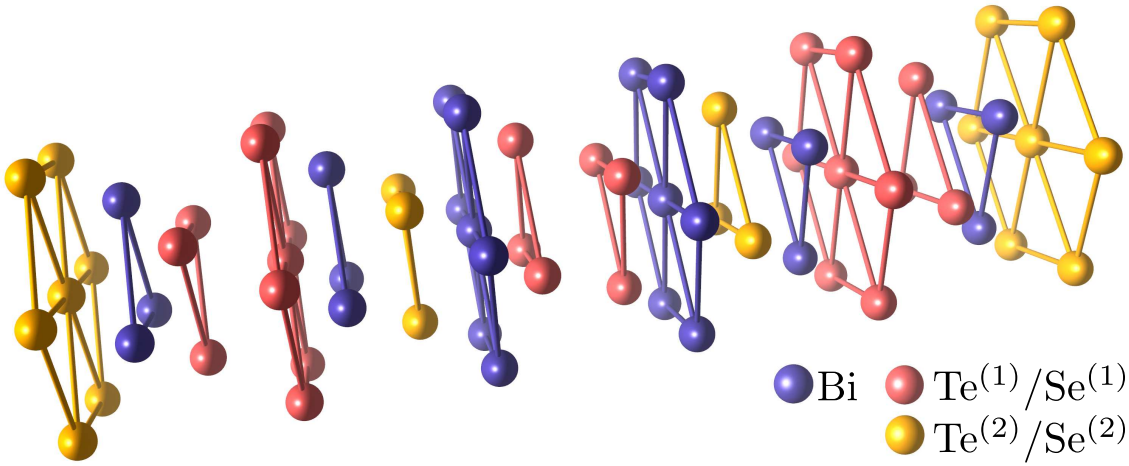

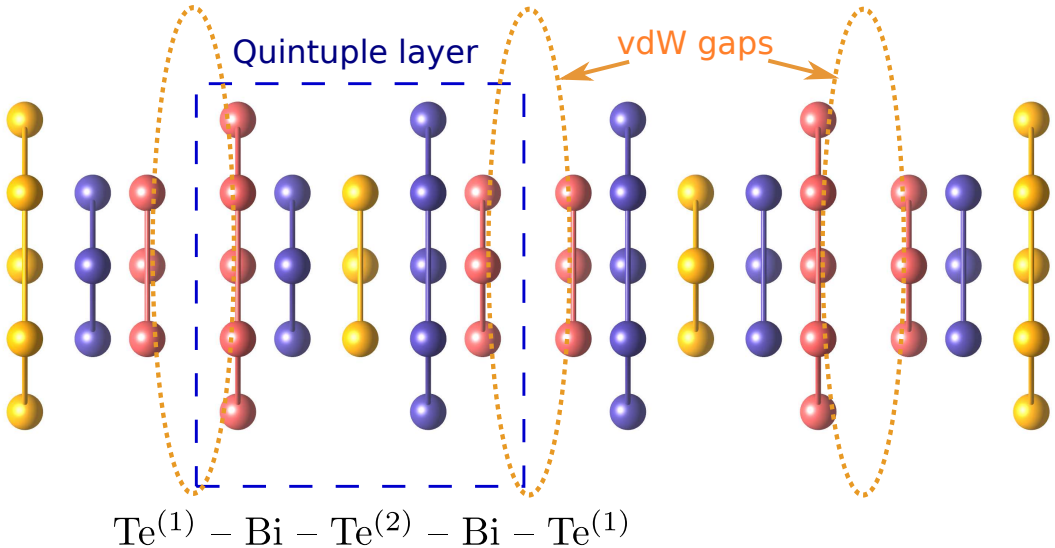

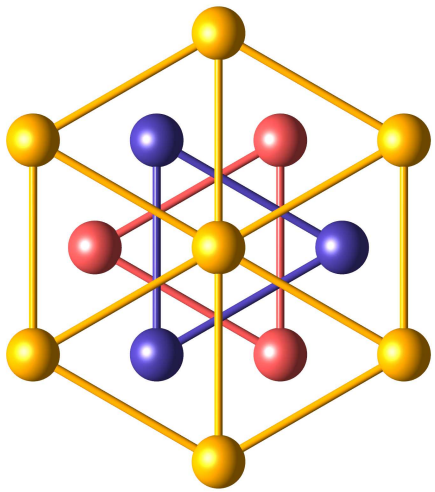

Band structure of 3D topological insulators

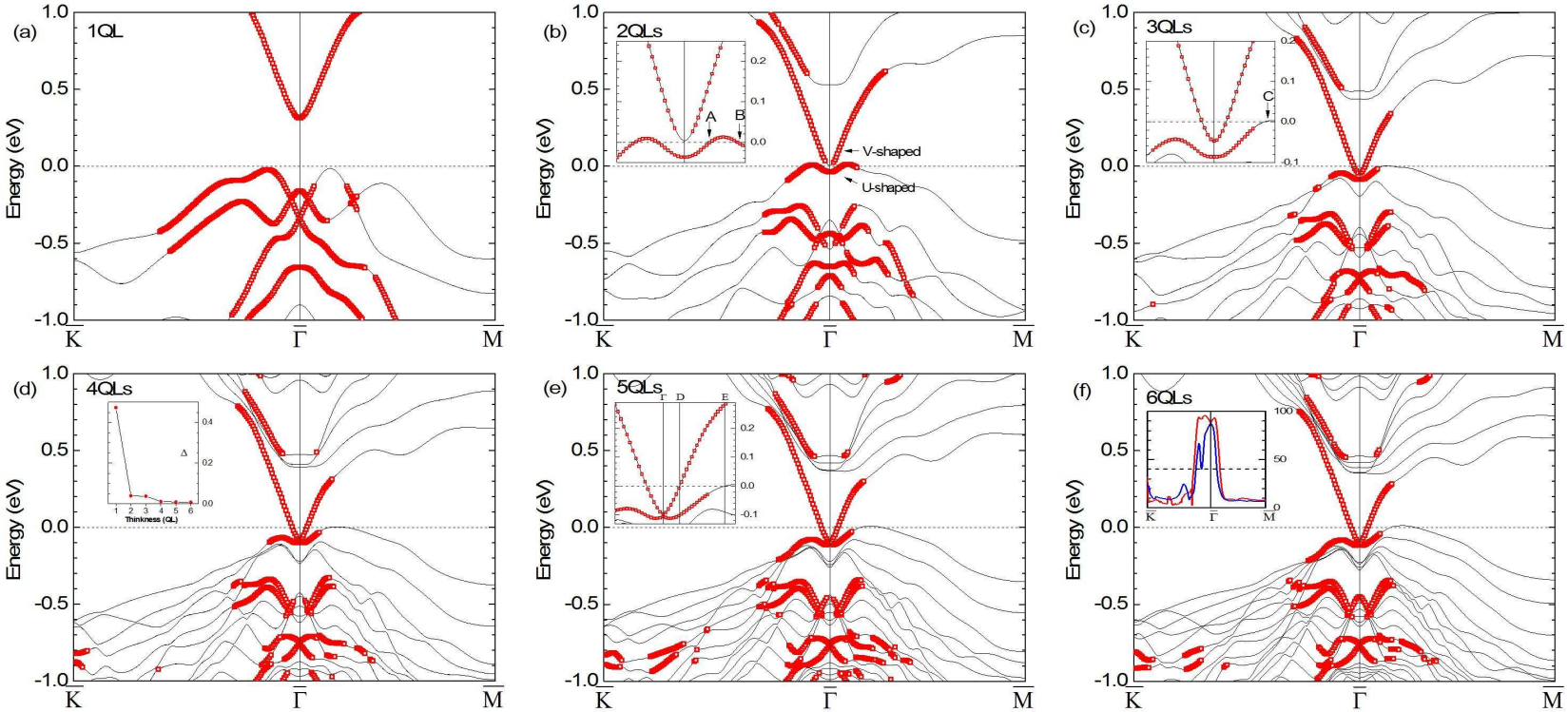

Xian-Qi Dai, Bao Zhao, Jian-Hua Zhao, *et al.*

Robust surface state of intrinsic topological insulator $Bi_2 Te_2 Se$ thin films: a first-principles study

J. Phys.: Cond. Mat. **24**, 035502 (2012)

Mn-doped Bi_2Te_3 and Bi_2Se_3

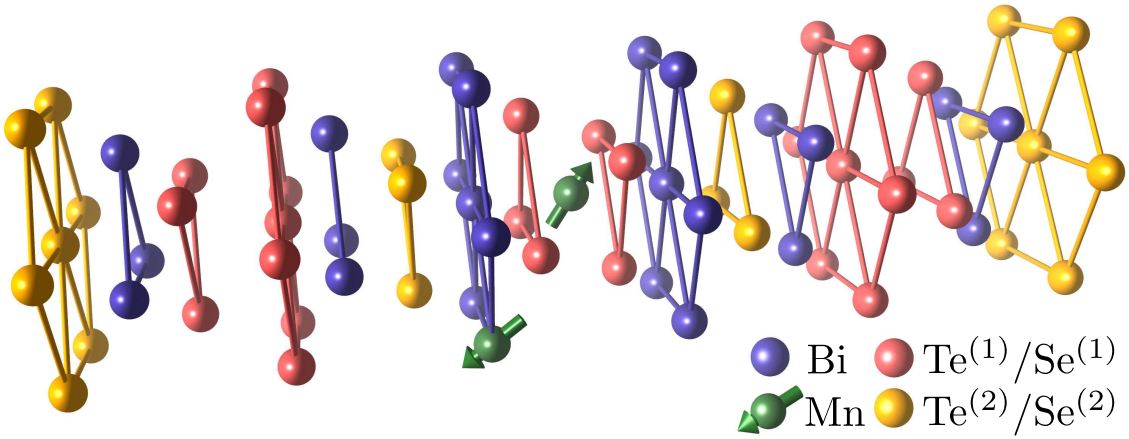

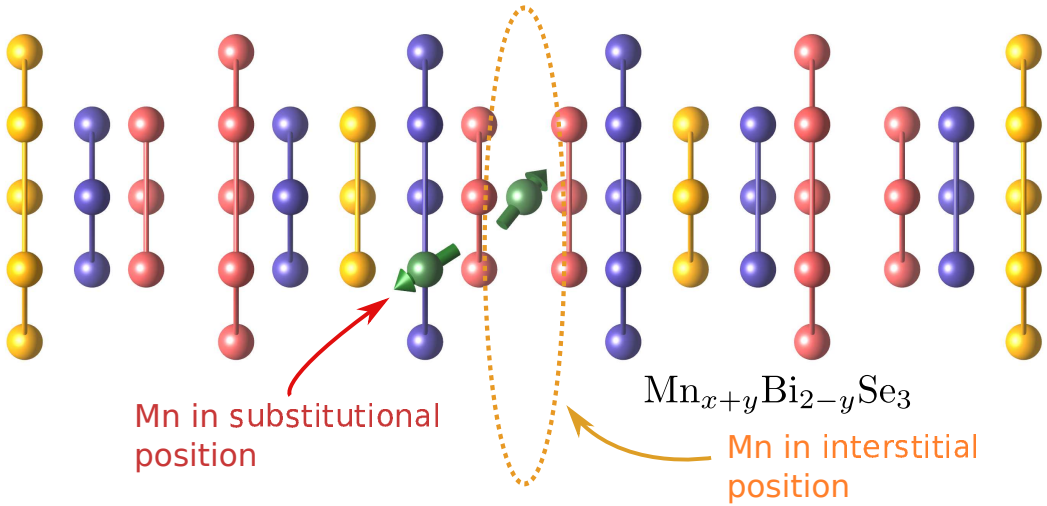

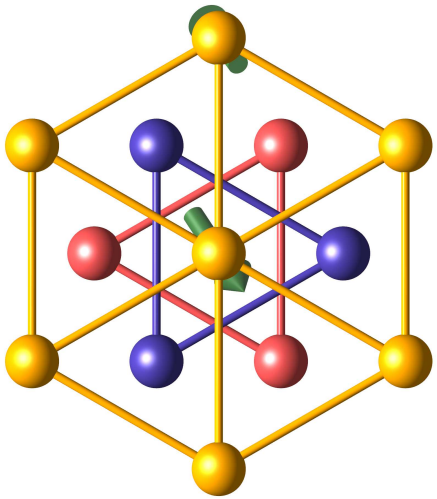

Mn-doped Bi_2Te_3 and Bi_2Se_3

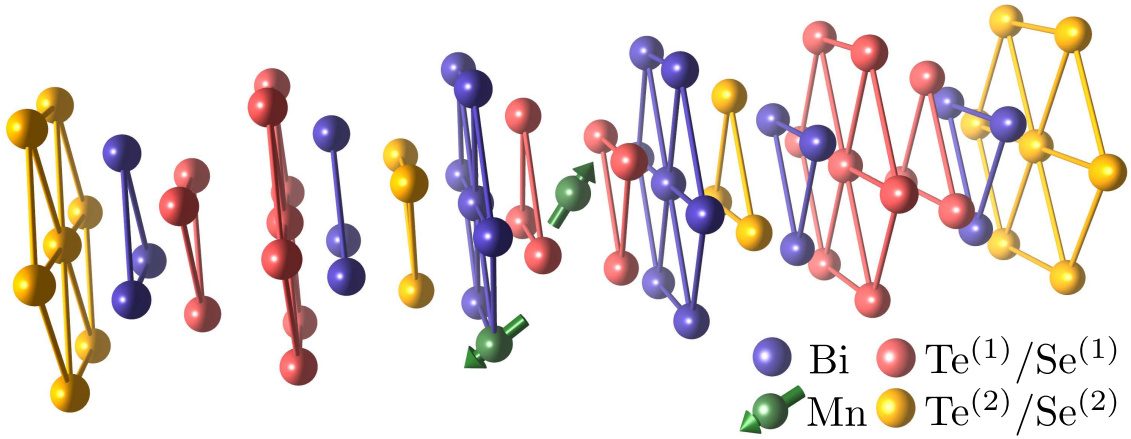

substitutional positions

- Mn-atom substitutes Bi
- *p-type* doping

intersitial positions

- Mn-atom in Van der Waals gap
- *n-type* doping

Y. S. Hor, P. Roushan, H. Beidenkopf, *et al.*
Development of ferromagnetism in dopped topological insulators $Bi_{2-x}Mn_xTe_3$
Phys. Rev. B **81**, 195203 (2010)

J. Růžička, O. Caha, V. Holý, *et al.*
Structural and electronic properties of manganese-doped Bi_2Te_3 epitaxial layers
New J. Phys. **17**, 013028 (2015)

Band structure of Bi_2Te_3 with spin-orbit interaction

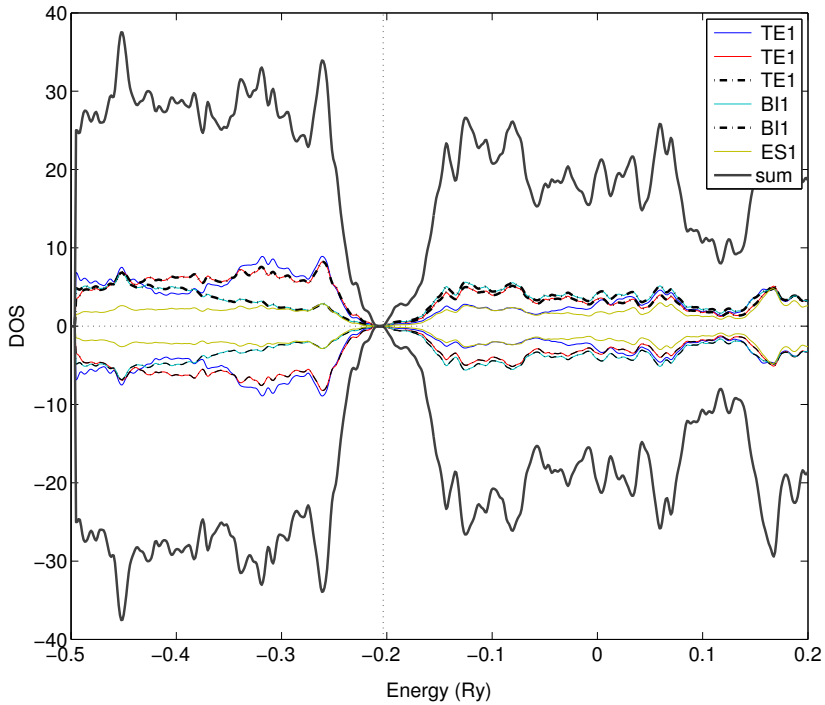

- bad gap is $0.11\ \mathrm{eV}$ (experimental value: $0.16\ \mathrm{eV}$)
- band gap vanishes without spin-orbit interaction

Mn-doped Bi_2Te_3: band structure

Substitutional Mn-atoms

$Bi_{2-x}Mn_xTe_3$, $0.02 < x < 0.18$

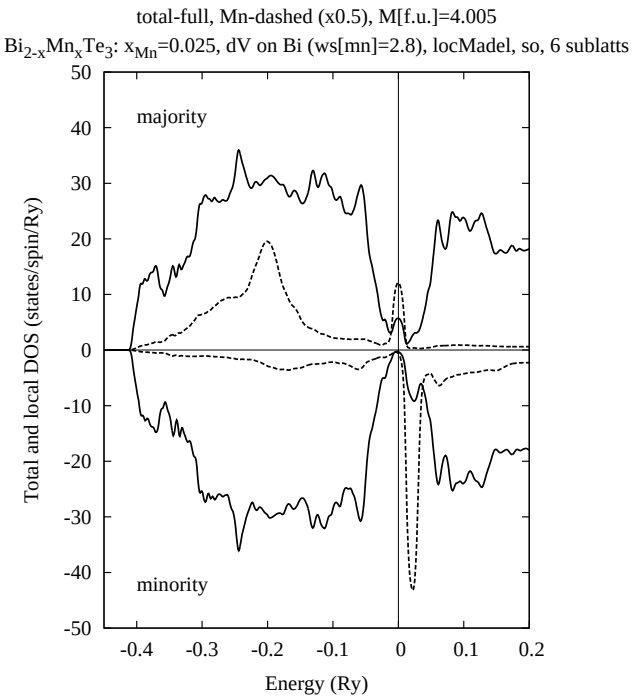

- Mn mag. moment: $3.36 - 3.43\,\mu_B$
- Fermi level in Mn-impurity peak in the majority spin channel

Interstitial Mn-atoms

$Mn_xBi_2Te_3$, $0.02 < x < 0.10$

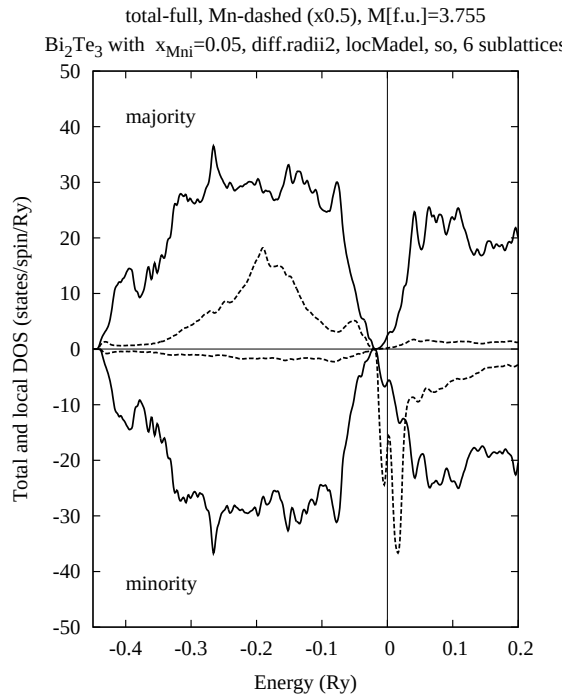

- Mn mag. moment: $3.53 - 3.65\,\mu_B$
- Fermi level is shifted to conduction band

Bulk conductivity of Mn-doped Bi_2Te_3

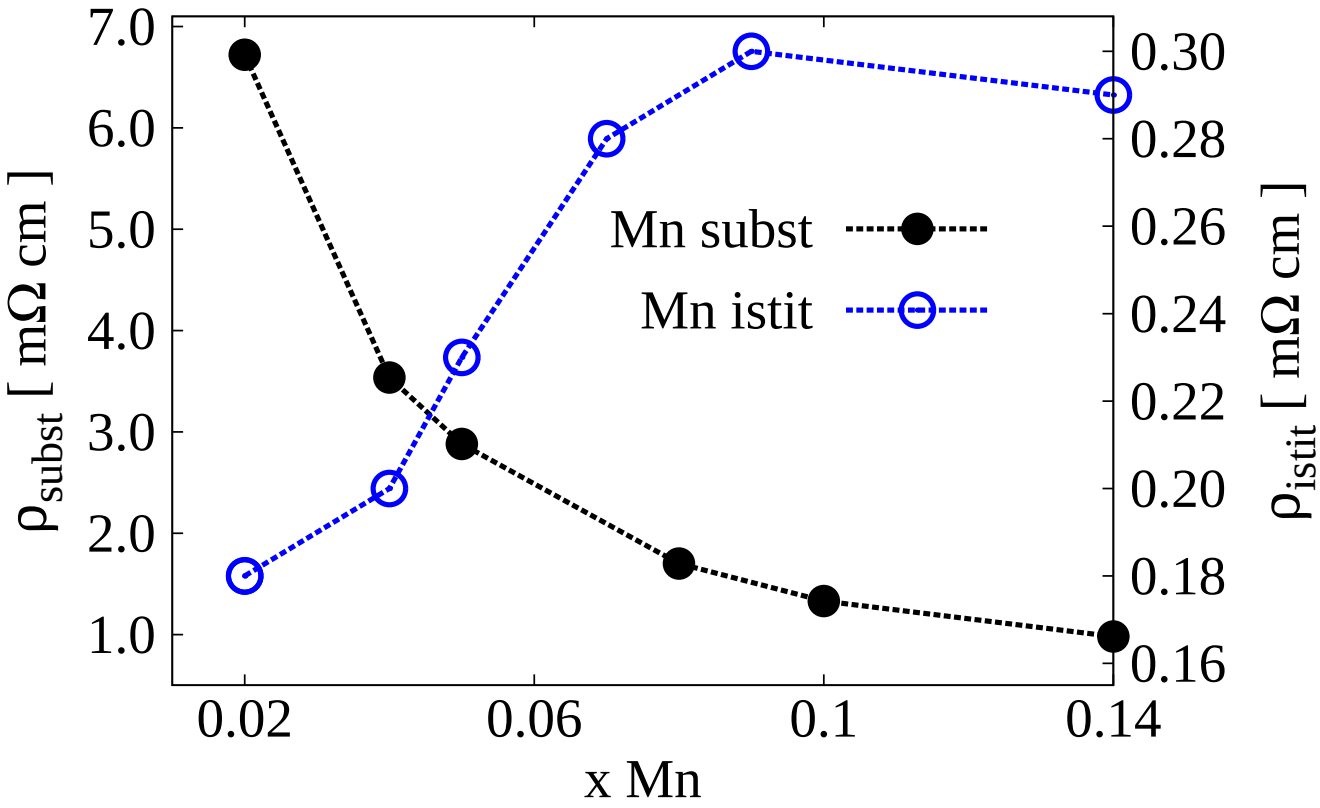

K. Carva, J. Kudrnovský, F. Máca, V. Drchal, I. Turek, P. Baláž, V. Tkáč, V. Holý, V. Sechovský, and J. Honolka

Electronic and transport properties of the Mn-doped topological insulator Bi_2Te_3 : A first-principles study

Phys. Rev. B **93**, 214409 (2016)*

* Selected for Phys. Rev. B Kaleidoscope, June 2016

Bulk conductivity of Mn-doped Bi_2Te_3

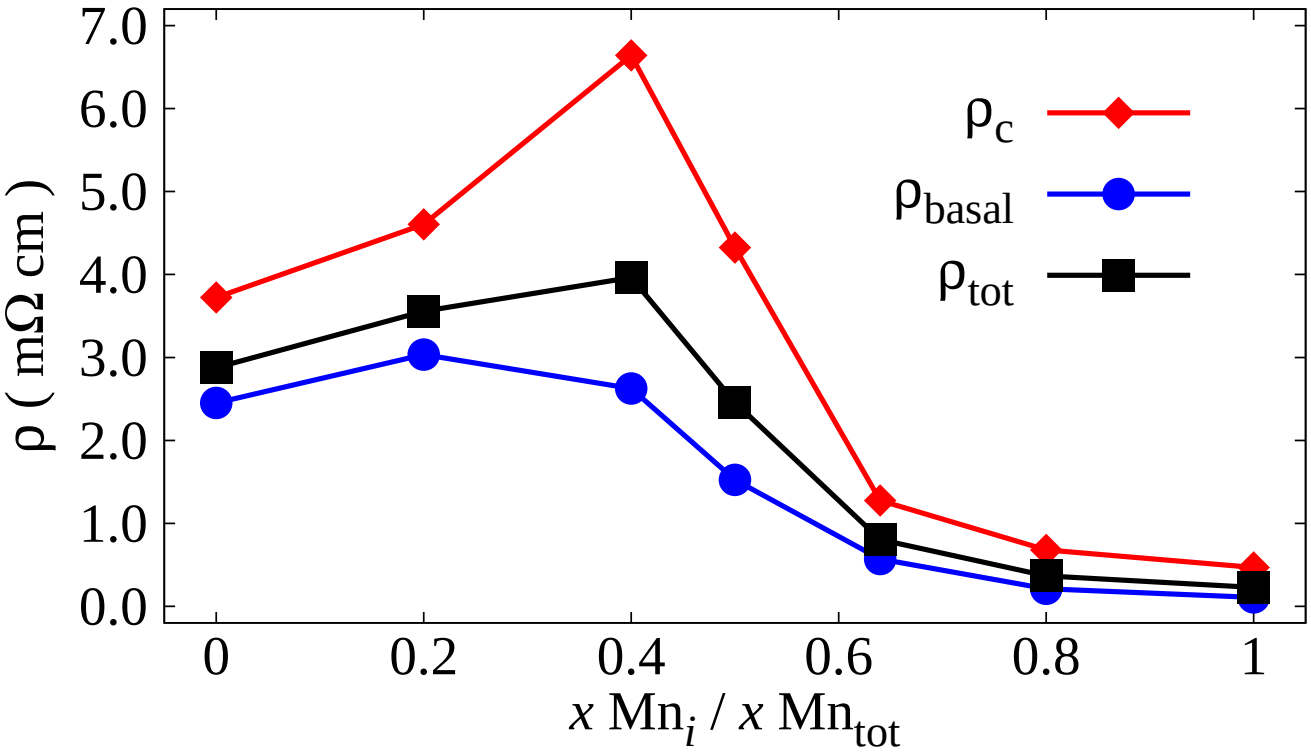

ρ_c along c-axis, ρ_{basal} parallel to basal plane, ρ_{tot} total resistivity

K. Carva, J. Kudrnovský, F. Máca, V. Drchal, I. Turek, P. Baláž, V. Tkáč, V. Holý, V. Sechovský, and J. Honolka
Electronic and transport properties of the Mn-doped topological insulator Bi_2Te_3 : A first-principles study
Phys. Rev. B **93**, 214409 (2016)*

* Selected for Phys. Rev. B Kaleidoscope, June 2016

Cr-doped Bi_2Te_3

Exchange interactions calculated for $p_{\mathrm{sub}} = 0.05$ and $p_{\mathrm{int}} = 0$

in the same sublattice

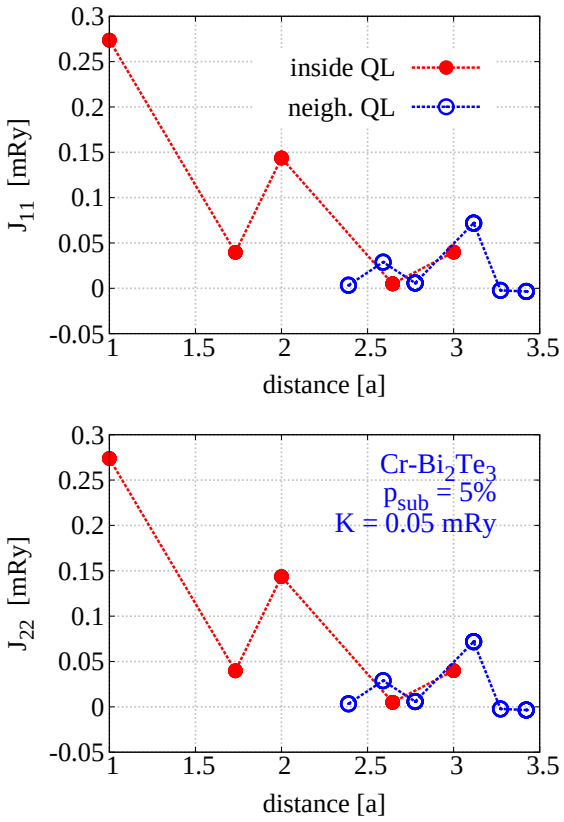

Cr-doped Bi_2Te_3

Exchange interactions calculated for $p_{\mathrm{sub}} = 0.05$ and $p_{\mathrm{int}} = 0$

in the same sublattice

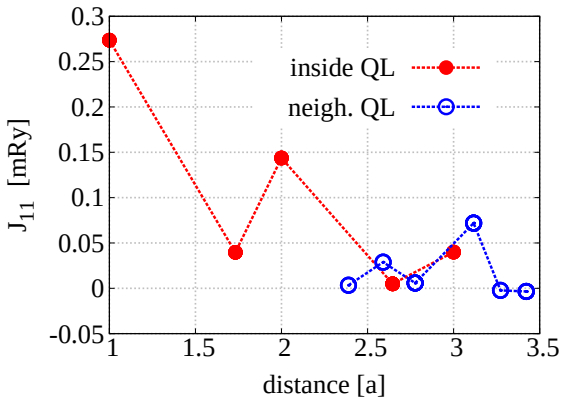

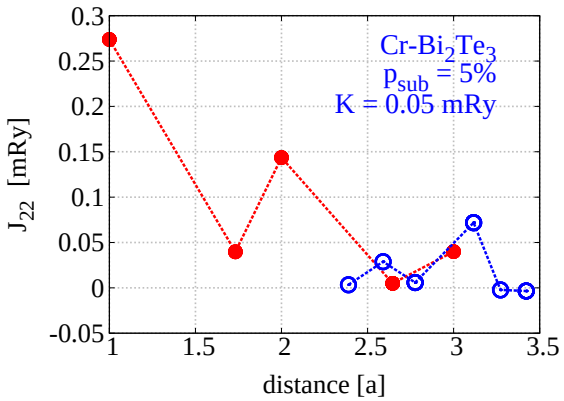

between different sublattices

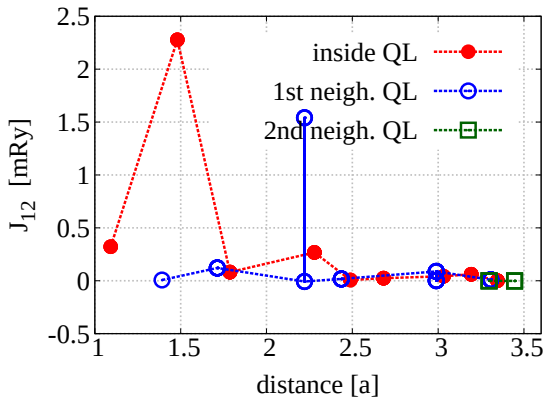

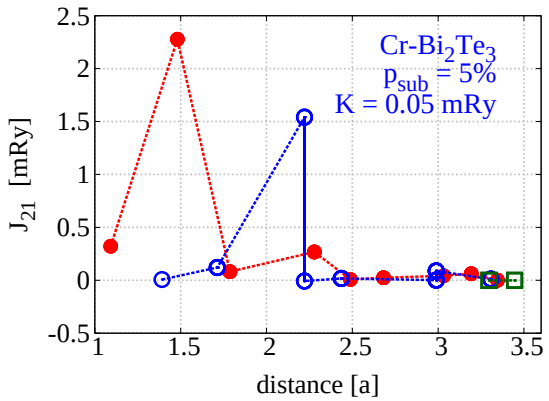

Studied quantities in atomistic simulations

- Magnetization

$$\boldsymbol{M} = \frac{1}{N}\sum_{i=1}^{N} \boldsymbol{m}_i$$

- Susceptibility

$$\chi = \frac{1}{N}\frac{\partial \left\langle M \right\rangle}{\partial H} = \frac{\left\langle M^2 \right\rangle - \left\langle M \right\rangle^2}{N k_{\mathrm{B}} T}$$

- Heat capacity

$$C = \frac{1}{N}\frac{\partial \left\langle E \right\rangle}{\partial T} = \frac{\left\langle E^2 \right\rangle - \left\langle E \right\rangle^2}{N k_{\mathrm{B}} T^2}$$

- Binder cumulant

$$U \equiv U(L, T) = 1 - \frac{\left\langle M^4 \right\rangle}{3\left\langle M^3 \right\rangle}$$

Studied quantities in atomistic simulations

- Magnetization

$$\boldsymbol{M} = \frac{1}{N}\sum_{i=1}^{N} \boldsymbol{m}_i$$

- Susceptibility

$$\chi = \frac{1}{N}\frac{\partial \langle M \rangle}{\partial H} = \frac{\langle M^2 \rangle - \langle M \rangle^2}{N k_{\mathrm{B}} T}$$

- Heat capacity

$$C = \frac{1}{N}\frac{\partial \langle E \rangle}{\partial T} = \frac{\langle E^2 \rangle - \langle E \rangle^2}{N k_{\mathrm{B}} T^2}$$

- Binder cumulant

$$U \equiv U(L, T) = 1 - \frac{\langle M^4 \rangle}{3 \langle M^3 \rangle}$$

Binder cumulant

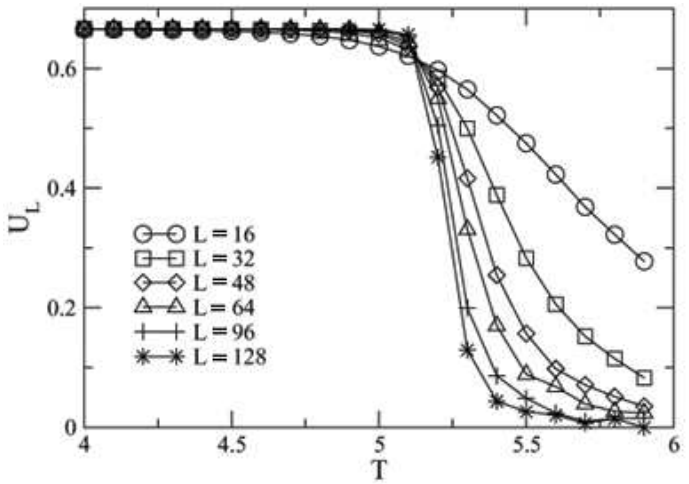

FIG. 2: Fourth-order Binder cumulants U_L versus temperature T, for various lattice sizes as indicated in the figure and for the point $h_r = 0$, $h = 1.0$. The erros bars are less than the size of the data points.

- for $T \to 0$, $U(L, T) \to 2/3$
- for $T \to \infty$, $U(L, T) \to 1/L$
- for $T = T_{\mathrm{c}}$, $U(L, T) = U_0$ for each L

Cr-doped Bi_2Te_3

$p_{\mathrm{sub}} = 10\%$, $p_{\mathrm{int}} = 0$ $(L = 40)$

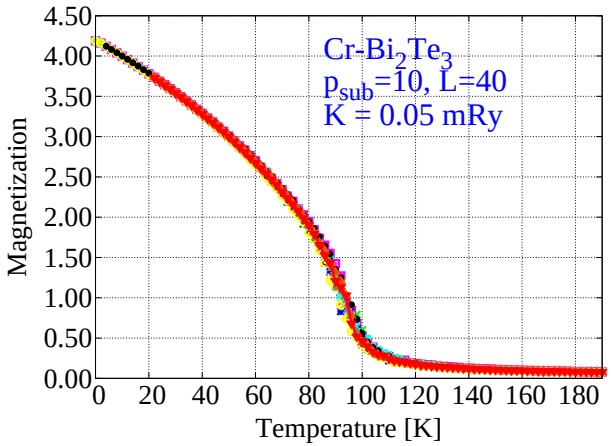

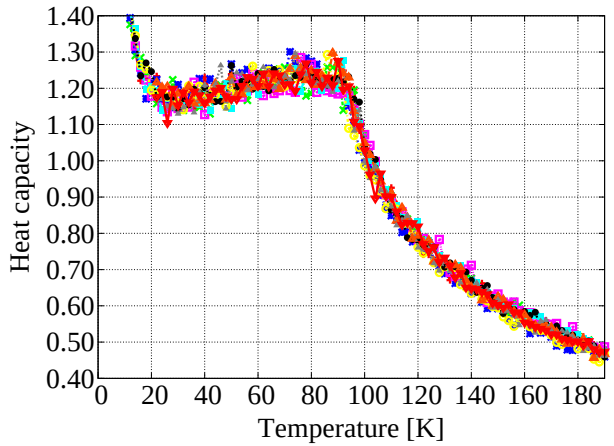

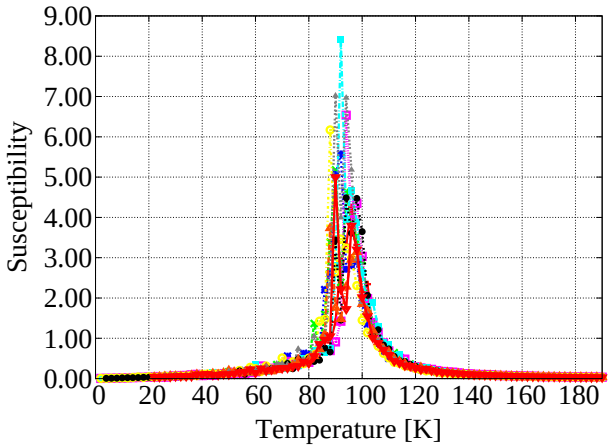

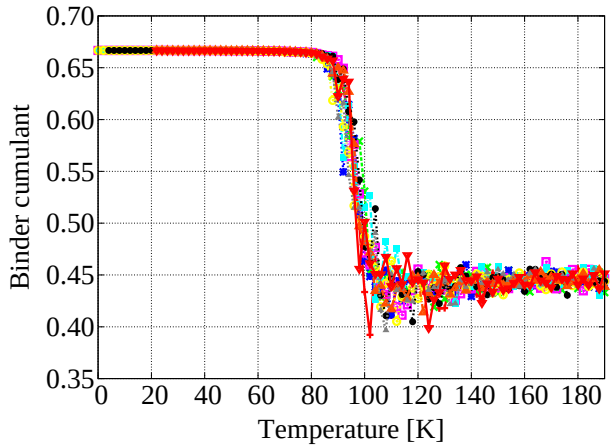

Cr-doped Bi_2Te_3

$p_{\mathrm{sub}} = 10\%$, $p_{\mathrm{int}} = 0$ $(L = 40)$

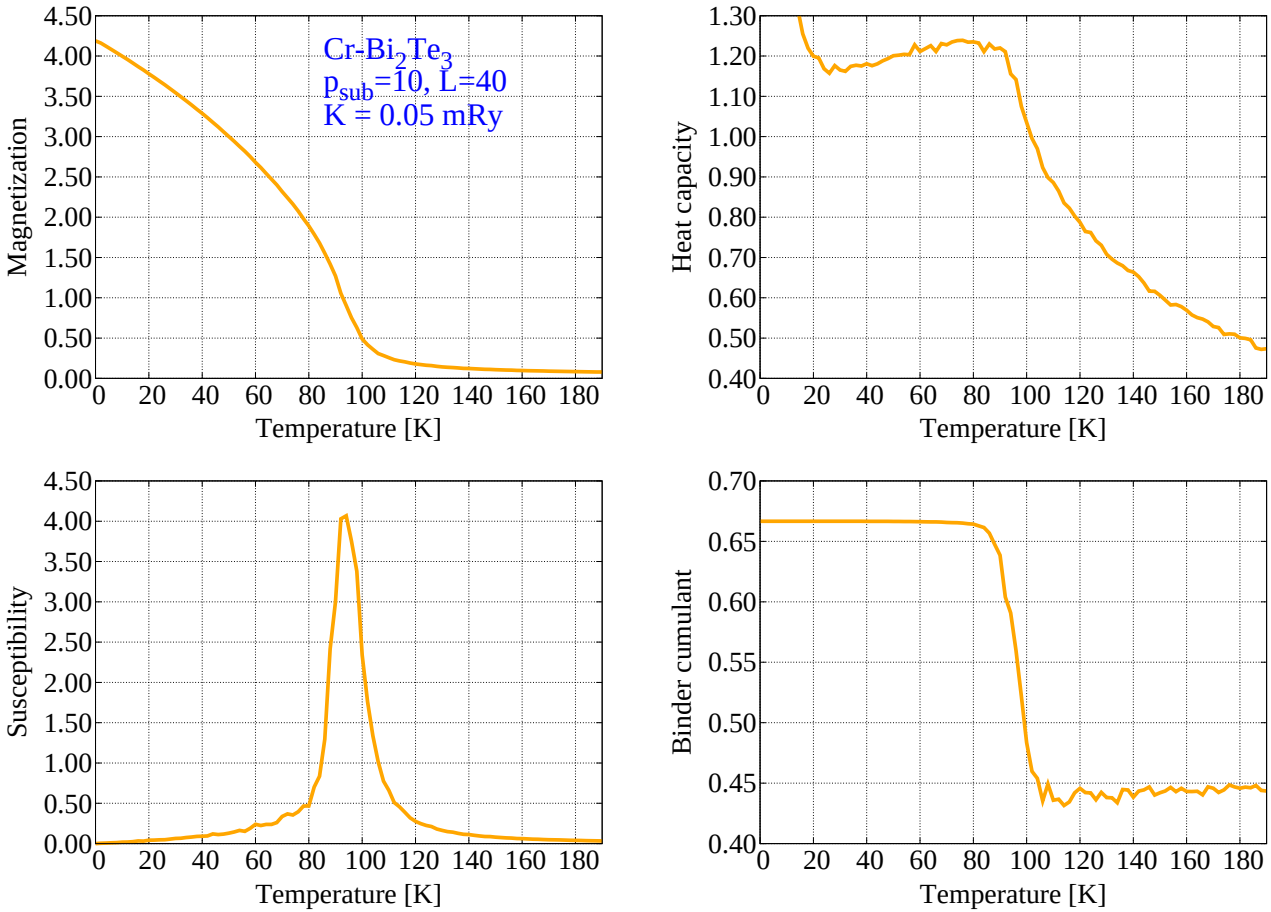

Cr-doped Bi_2Te_3

$p_{\mathrm{sub}} = 10\%$, $p_{\mathrm{int}} = 0$

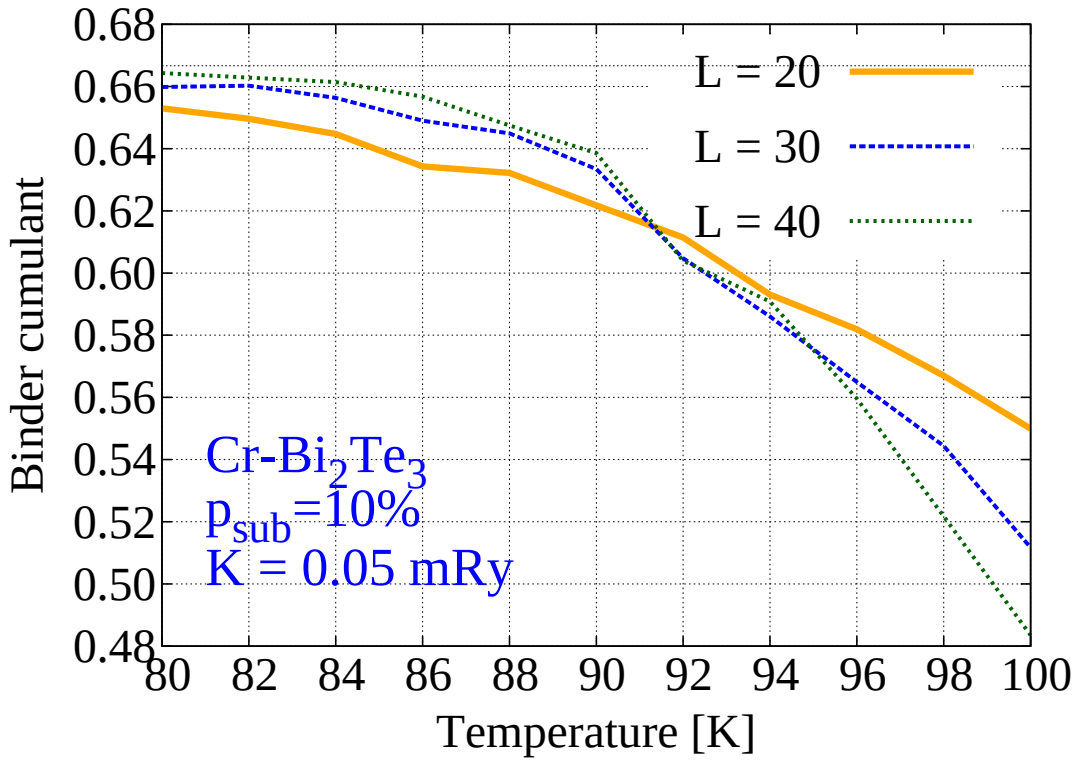

$T_{\mathrm{c}} = 91\,\mathrm{K}$

Cr-doped Bi_2Te_3

Currie temparature *vs.* Cr concentration

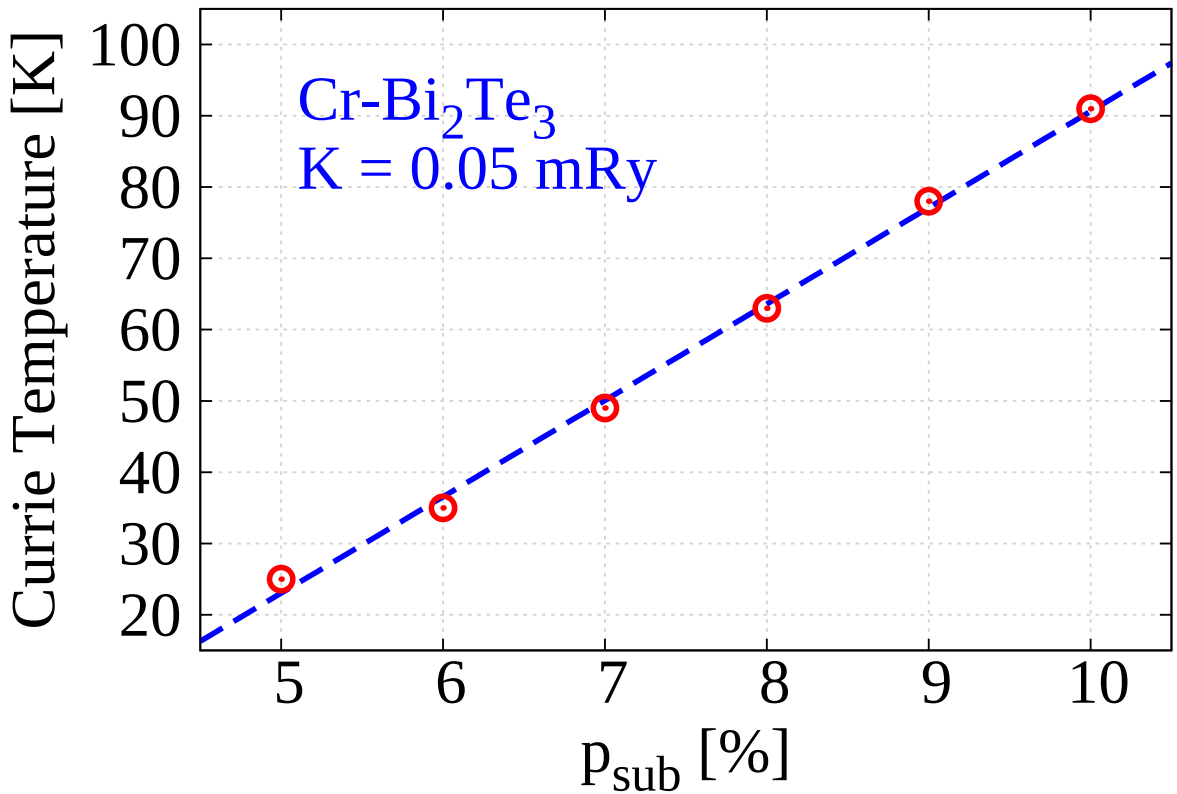

Mn-doped Bi_2Se_3

Currie temparature *vs.* Mn concentration

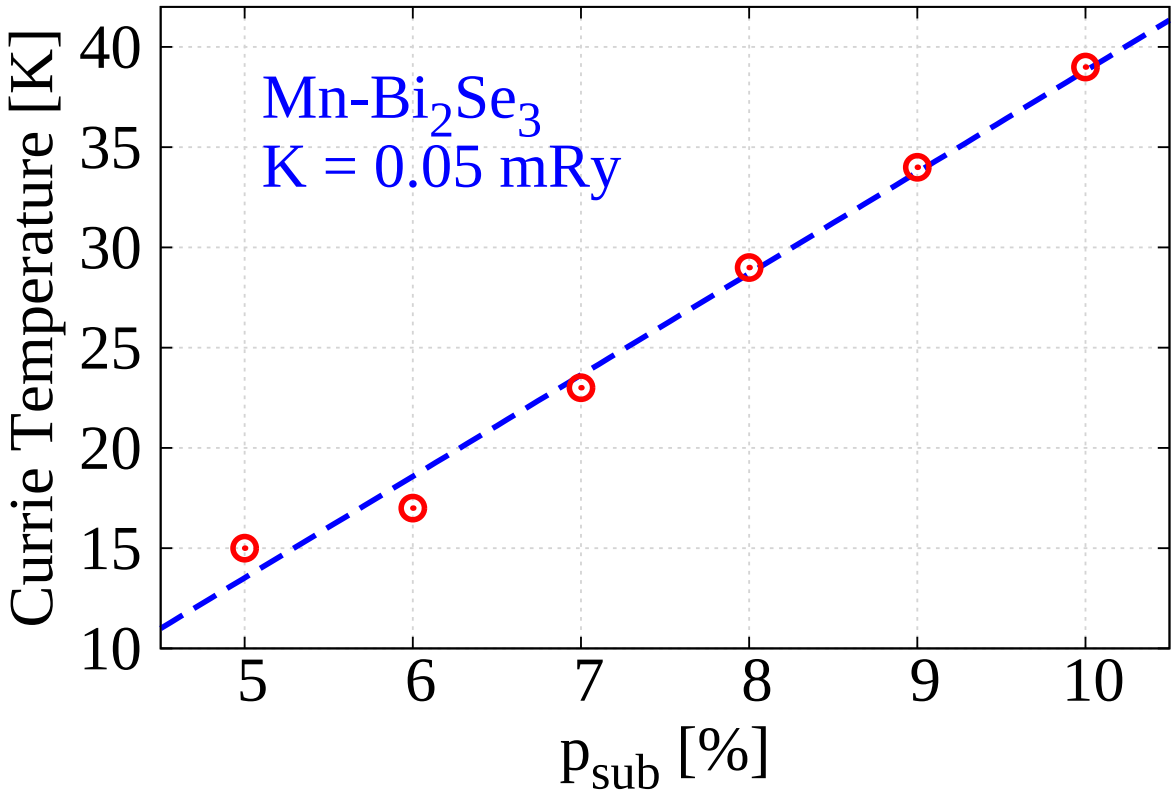

Summary

- Although exchange interactions between QLs are smaller than those inside QL, they influence the value of T_c
- Currie temperature depends on the type of Mn atoms in Bi_2Se_3 (interstitial and substitutional)
- Currie temperature of 3D topological insulators might be taylored by means of concentrations of both Mn atoms types

Outline

Laser-pulse-induced ultrafast demagnetization

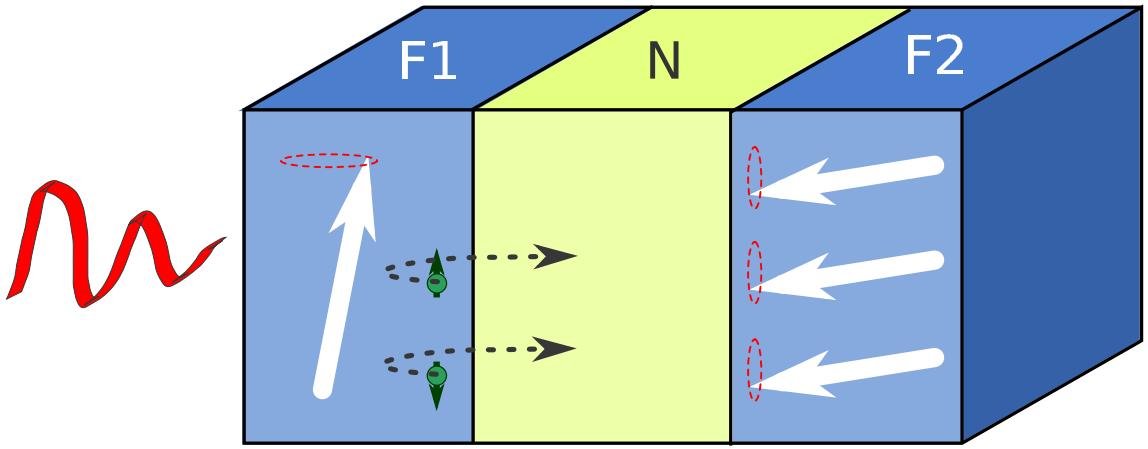

Laser-pulse-induced ultrafast demagnetization

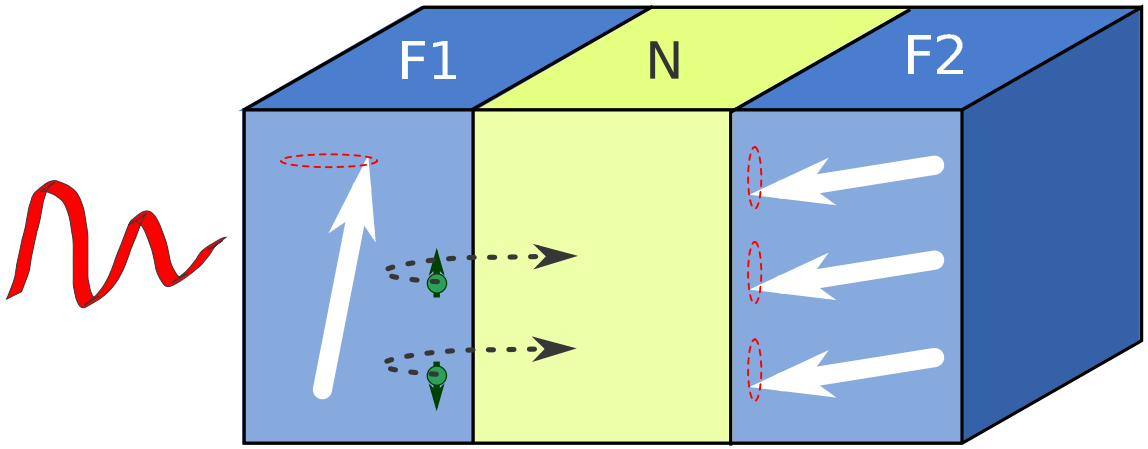

Ultrafast demagnetization in F1

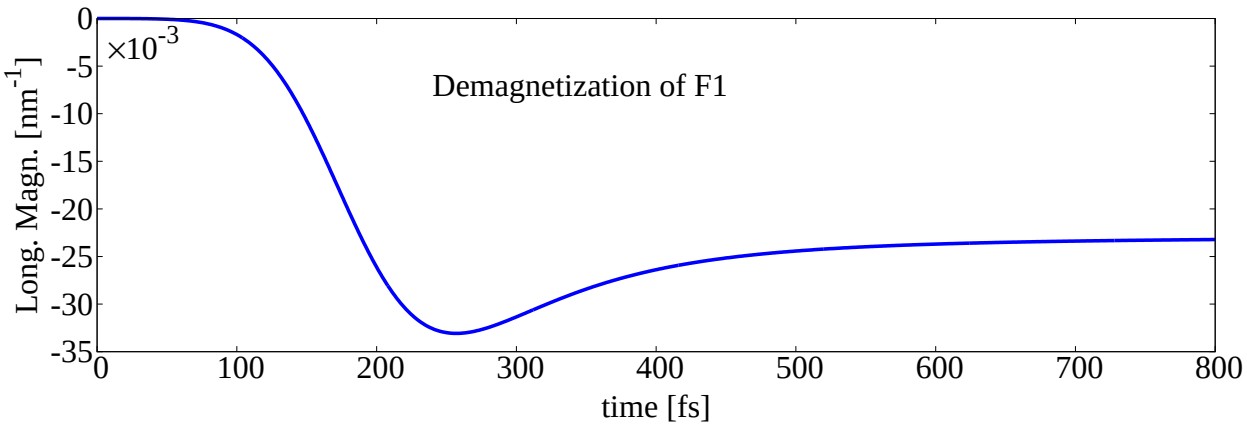

Laser-pulse-induced ultrafast magnetization dynamics in F2

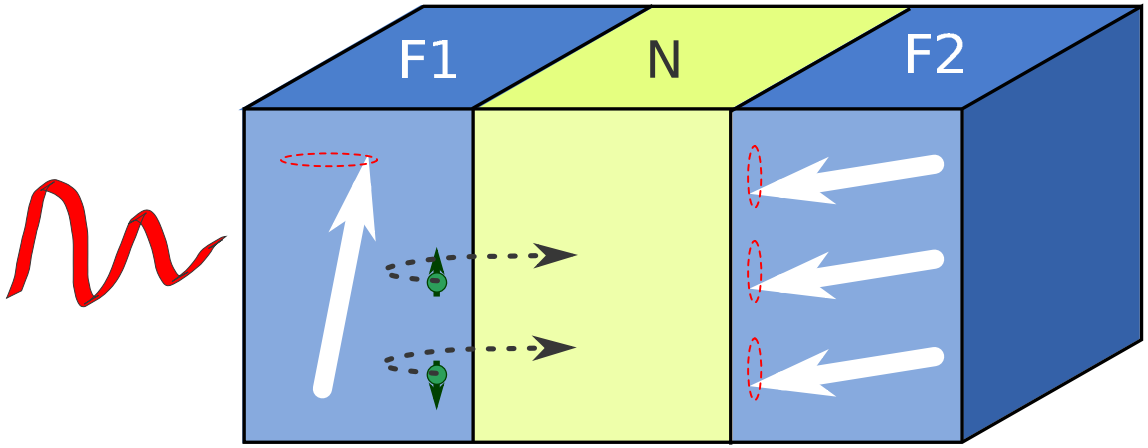

A.J. Schellekens, K.C. Kuiper, R.R.J.C. de Wit, and B. Koopmans

Ultrafast spin-transfer torque driven by femtosecond pulsed-laser excitation
Nature Communications 5, 4333 (2014)

Theoretical framework

Superdiffusive spin transport of hot electrons

M. Battiato, K. Carva, and P. M. Oppeneer

Superdiffusive Spin Transport as a Mechanism of Ultrafast Demagnetization
Phys. Rev. Lett. 105, 027203 (2010)

- One solves a diffusion-like equation for spin densities $n_{\uparrow(\downarrow)}$ in two-channel model

$$n_{\uparrow(\downarrow)}(z, t+\delta t) = e^{-\delta t/\tau_{\uparrow(\downarrow)}(z)}\, n_{\uparrow(\downarrow)}(z, t) + S^{e}_{\uparrow(\downarrow)}(z, t+\delta t) + \Phi_{\uparrow(\downarrow)}$$

with the spin-dependent total effective source

$$S^{e}_{\uparrow(\downarrow)}(z, t+\delta t) = S_{\uparrow(\downarrow)}(z, t+\delta t) + S^{p}_{\uparrow(\downarrow)}(z, t+\delta t)$$

where $S_{\uparrow(\downarrow)}(z, t+\delta t)$ is an external contribution

- $S^{p}_{\uparrow(\downarrow)}(z, t+\delta t)$ is a contribution due to electrons relaxation from energy level ϵ' with spin σ'

$$S^{p}_{\sigma}(\epsilon, z, t+\delta t) = \sum_{\sigma'} \int_{0}^{\epsilon_{\max}} \mathrm{d}\epsilon'\; n_{\sigma'}(\epsilon', z, t)\, p_{\sigma',\sigma}(\epsilon', \epsilon, z, t) \left(1 - e^{-\delta t/\tau_{\sigma'}(\epsilon', z, t)}\right)$$

- the integrated flux reads

$$\Phi_{\uparrow(\downarrow)} = \sum_{t_0=0}^{t} \sum_{z_0} S^{e}_{\uparrow(\downarrow)}(z_0, t_0) \left[\psi^{-}_{\uparrow(\downarrow)}(z, t|z_0, t_0) - \psi^{+}_{\uparrow(\downarrow)}(z, t|z_0, t_0)\right]$$

Simple spin torque model

- Calculate spin density in a two channel model in a collinear configuration
- Assume that in case of noncollinear configuration transverse spin components are absorbed directly at the N/F2 interface
- Absorbed spin flux is transformed into spin transfer torque

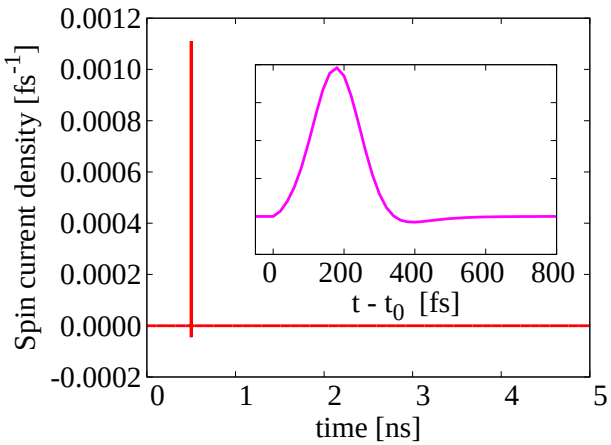

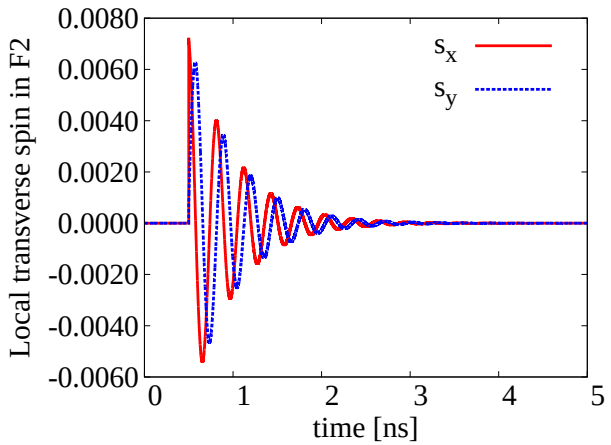

Matrix formalism

- The spin density in a matrix form $\check{n} = n_0\,\sigma_0 + \boldsymbol{n}\cdot\boldsymbol{\sigma}$ where $\boldsymbol{n} = (n_x, n_y, n_z)$

$$\check{\boldsymbol{n}}(z, t+\delta t) = e^{-\delta t/\tau_0}\,\check{\boldsymbol{n}}(z,t) + \check{\boldsymbol{S}}^e(z, t+\delta t) + \check{\boldsymbol{\Phi}}(z,t)$$

  where $\check{\boldsymbol{S}}^e(z,t) = S_0^e\,\sigma_0 + \boldsymbol{S}^e\cdot\boldsymbol{\sigma}$, and $\check{\boldsymbol{\Phi}}(z,t) = \Phi_0\,\sigma_0 + \boldsymbol{\Phi}\cdot\boldsymbol{\sigma}$.

- with particle and spin sources

$$S_0^e(z, t+\delta t) = S_0(z, t+\delta t) + \left(1 - e^{-\delta t/\tau(z)}\right)\,p(z)\,n_0(z,t)$$

$$\boldsymbol{S}^e(z, t+\delta t) = \boldsymbol{S}(z, t+\delta t) + \left(1 - e^{-\delta t/\tau(z)}\right)\,p(z)\,\boldsymbol{n}(z,t)$$

  where $\boldsymbol{S} = (S_x, S_y, S_z)$

- and particle and spin fluxes

$$\Phi_0(z,t) = \sum_{t_0=0}^{t}\sum_{z_0} S_0^e(z_0,t_0)\left[\psi^-(z,t|z_0,t_0) - \psi^+(z,t|z_0,t_0)\right]$$

$$\boldsymbol{\Phi}(z,t) = \sum_{t_0=0}^{t}\sum_{z_0} \boldsymbol{S}^e(z_0,t_0)\left[\psi^-(z,t|z_0,t_0) - \psi^+(z,t|z_0,t_0)\right]$$

Open questions

- Treatment of transport of the hot electrons through the interfaces
- Treatment of hot electrons inside the ferromagnetic layer
- How to improve the magnetization dynamics and induce light-induced switching?

SWISS CONTRIBUTION

NANOSPIN

Thank you for your attention

AGH

ÉCOLE POLYTECHNIQUE FÉDÉRALE DE LAUSANNE

IF PAN